HIGH GLUCOSE-INDUCED ROS PRODUCTION IS MEDIATED BY C-SRC IN MESANGIAL CELLS

by

Ken W.K. Lee

A thesis submitted in conformity with the requirements
for the degree of Master of Science
Graduate Department of Physiology
University of Toronto

Library and Archives Canada

Published Heritage Branch

395 Wellington Street
Ottawa ON K1A 0N4
Canada

Bibliothèque et Archives Canada

Direction du Patrimoine de l'édition

395, rue Wellington
Ottawa ON K1A 0N4
Canada

Your file Votre référence
ISBN: 978-0-494-85876-9

Our file Notre référence
ISBN: 978-0-494-85876-9

ABSTRACT

Ken W. K. Lee

Master of Science (2011)

Graduate Department of Physiology

University of Toronto

HIGH GLUCOSE-INDUCED ROS PRODUCTION IS MEDIATED BY C-SRC IN MESANGIAL CELLS

The pathogenesis of diabetic nephropathy (DN) remains incompletely understood. In previous studies, we observed the activation of Src by high glucose (HG) and showed that Src is required for MAPK activation and synthesis of collagen IV in cultured rat mesangial cells (MCs). Reactive oxygen species (ROS) are also important mediators of DN, and our present study aimed to investigate the role of Src in HG-induced ROS generation. In MCs, we found that HG led to ROS accumulation that was blocked by Src inhibitors or Src-specific siRNA. Downstream of Src, Vav2 was phosphorylated/activated leading to Rac1-dependent NADPH oxidase activation. Long-term HG exposure resulted in Src-dependent Nox4 protein induction. Nox2-specific siRNA abrogated ROS production only in short-term HG, while Nox4-specific siRNA blocked ROS production only in long-term HG. Taken together, our data indicate Src to be important in mediating ROS generation from both Nox2- and Nox4-containing NADPH oxidases.

ACKNOWLEDGEMENTS

First, I would like to thank my supervisor and mentor, Dr. I. George Fantus, for his guidance and support during my graduate training. As a Master's student, I have undoubtedly matured as a scientist in several regards. Dr. Fantus provided expertise in the field of diabetes and nephropathy, assisted in troubleshooting experimental protocols, and trained me to becoming an effective scientific communicator. Being a researcher and a clinician, Dr. Fantus' demeanor and professionalism are qualities I aspire to attain as I pursue a future career in medicine.

I would also like to thank my supervisory committee, Dr. Adria Giacca and Dr. Jonathan Rocheleau, for their positive feedback and expertise in my Master's project. I appreciate all their advice, which enabled me to successfully complete my research project as smoothly as possible.

I would like to thank former and current members of the Fantus lab for their support. In particular, I am deeply grateful for Ling Xia for her technical support and guidance in the lab. She also laid the groundwork for the Src project, providing preliminary and animal data relating to my current project. I appreciate the help given by Howard Goldberg and Anu Shah, who investigated other aspects of diabetic nephropathy. I would like to thank Chester Yao, a summer student from 2010, for helping with some of the experiments.

Last but not least, I would like to thank my family and friends for their moral support. My parents have stuck by me through my undergraduate and graduate years in the medical sciences, and now support my decision to apply for

medical school. I appreciate my friends for always being there for me, and I truly enjoy their company.

TABLE OF CONTENTS

LIST OF PUBLICATIONS AND PRESENTATIONS

Publications-

- Taniguchi, K., Xia, L., Goldberg, H., Lee, K.W.K., Whiteside, C., and Fantus, I.G. Inhibition of Src Kinase Blocks High Glucose-Induced EGFR Transactivation and Collagen Synthesis in Mesangial Cells and Prevents Diabetic Nephropathy in Mice. *Submitted to the journal Diabetes and returned for revisions*.
- Lee, K.W.K., Xia, L., Goldberg, H., Whiteside, C., and Fantus, I.G. High Glucose-Induced ROS production is Mediated by C-Src in Mesangial Cells. *Manuscript in progress*.

Oral Presentations-

- "High glucose-induced ROS production is mediated by c-Src in mesangial cells" presented at UHN / Lunenfeld Institute Diabetes Seminar on December 10, 2010, at MaRS Centre Toronto Medical Discovery Tower (TMDT) 4-204

Poster Presentations-

- "High glucose-induced ROS production is mediated by c-Src in mesangial cells" poster presented at:
    - Frontiers in Physiology on April 8, 2011, at Medical Sciences Building, University of Toronto
    - Banting and Best Diabetes Centre Scientific Day on May 13, 2011, at The Old Mill Inn
    - Samuel Lunenfeld Research Institute Retreat Poster Session on May 16, 2011, at YMCA Geneva Park
    - ENDO2011 Conference on June 4, 2011, at Boston Convention and Exhibition Centre, Boston, MA
    - Endocrinology and Diabetes Research Group (EDRG) Scientific Day on June 16, 2011, at Medical Sciences Building, University of Toronto. **Awarded 2nd prize for poster session.**

LIST OF FIGURES

LIST OF ABBREVIATIONS

ACE	Angiotensin converting enzyme
AGEs	Advanced glycation end-products
Amino acid abbreviations:	
Arg	Arginine
Cys	Cysteine
E	Glutamic acid
Glu	Glutamic acid
I	Isoleucine
L	Leucine
P	Proline
pTyr/pY	Phosphorylated tyrosine
Tyr	Tyrosine
V	Valine
X	Any amino acid
Y	Tyrosine
ANOVA	Analysis of variance
ARB	Angiotensin receptor blocker
ARE	Antioxidant response element
AT_1R	Angiotensin II type I receptor
ATP	Adenosine triphosphate
BMK1	Big map kinase 1
BSA	Bovine serum albumin
CH domain	Calponin-homology domain
CM-H_2DCFDA	Chloromethyl-2',7'-dichlorodihydrofluorescein diacetate
Csk	C-terminal Src kinase
CTGF	Connective tissue growth factor
CuZnSOD	Copper-zinc superoxide dismutase
DAG	Diacylglycerol
DCF	2',7'-dichlorofluorescein
DH domain	Dbl-homology domain
DHE	Dihydroethidium
DMEM	Dulbecco's Modified Eagle Medium
DN	Diabetic nephropathy
DPI	Diphenyliodonium
DRIs	Direct renin inhibitors
DTT	Dithiothreitol
ECM	Extracellular matrix
EDTA	Ethylenediaminetetraacetic acid
EGTA	Ethylene glycol tetraacetic acid
EMT	Epithelial-to-mesenchymal transition
ERK1/2	Extracellular signal-regulated kinase 1/2
ESRD	End-stage renal disease
ETC	Electron transport chain

$FADH_2$	Flavin adenine dinucleotide (reduced form)
FBS	Fetal bovine serum
GAPs	GTPase activating proteins
GBM	Glomerular basement membrane
GDIs	GDP dissociation inhibitors
GEFs	Guanine exchange factors
GFB	Glomerular filtration barrier
GFR	Glomerular filtration rate
GTP	Guanosine triphosphate
GTPase	Guanosine triphosphatase
HEPES	4-(2-hydroxyethyl)-1-piperazineethanesulfonic acid
HG	High glucose
HIF-1α	Hypoxia inducible factor-1α
HO-1	Heme oxygenase-1
IgG	Immunoglobulin G
IU	International unit
MAPK	Mitogen-activated protein kinase
MCs	Mesangial cells
MCP-1	Monocyte chemoattractant protein-1
MICRO-HOPE	Heart Outcomes Prevention Evaluations (Renal Substudy)
MnSOD	Manganese superoxide dismutase
MR	Mineralocorticoid receptor
NADH	Nicotinamide adenine dinucleotide (reduced form)
NADPH	Nicotinamide adenine dinucleotide phosphate (reduced form)
NFκB	Nuclear factor kappa B
NIH	National Institute of Health
NOXA1	Nox activator 1
NOXO1	Nox organizer 1
Nrf2	Nuclear factor-erythroid 2-related factor-2
PAGE	Polyacrylamide gel electrophoresis
PAI-1	Plasminogen activator inhibitor-1
PAK	p21-activated protein kinase
PBS	Phosphate buffered saline
PDGF	Platelet-derived growth factor
PDK-1	Phosphoinositide-dependent kinase-1
PH domain	Pleckstrin-homology domain
PI3K	Phosphatidylinositol 3-kinase
PIP_2	Phosphatidylinositol-4,5-bisphosphate
PIP_3	Phosphatidylinositol-3,4,5-trisphosphate
PKC	Protein kinase C
PTP-α	Protein tyrosine phosphatase-α

qRT-PCR	Quantitative Reverse Transcription-Polymerase Chain Reaction
RAGE	Receptor for advanced glycation end-products
RAS	Renin angiotensin system
RLUs	Relative light units
ROS	Reactive oxygen species
SDS	Sodium dodecyl sulfate
SFK	Src family kinase
SH domain	Src-homology domain
SHP-2	SH2-containing protein tyrosine phosphatase-2
siRNA	Small interfering RNA
Smad1	Mothers against decapentaplegic homolog 1
STZ	Streptozotocin
TβR-I	TGF-β type I receptor
TβR-II	TGF-β type II receptor
TGF-β	Transforming growth factor-β
UCP-1	Uncoupling protein-1
VEGF	Vascular endothelial growth factor
ZF domain	Zinc finger domain

CHAPTER 1

INTRODUCTION

Chapter 1. Introduction

1.01 Diabetic Nephropathy

The worldwide prevalence of diabetes mellitus continue to increase at an alarming rate, with an estimated 171 million patients diagnosed in 2000 and is expected to reach 366 million by 2030 [1]. Chronic complications of diabetes continue to be major causes of severe illness, and renal disease is one of the most serious [2]. Indeed, the leading cause of end-stage renal disease (ESRD) requiring dialysis and transplantation is diabetic nephropathy (DN) [3]. It is predicted that the prevalence of ESRD arising from diabetes will increase by 70% by 2015 primarily due to an increase in the prevalence of diabetes rather than individual risk [4].

Structural changes associated with DN occur in many renal components, including the glomerular basement membrane (GBM), mesangium, podocytes and tubulointerstitial space [5] (Figure 1-1). Extracellular matrix (ECM) accumulation is a hallmark of DN, and is characterized by both an increase in normal ECM components such as type IV collagen, laminin and fibronectin [6] and atypical ECM components like type I and III collagen [7]. The GBM is a layer of ECM located between glomerular endothelial cells and podocytes, and is thought to have a direct role in filtration but also functions as a support structure for podocytes [8].

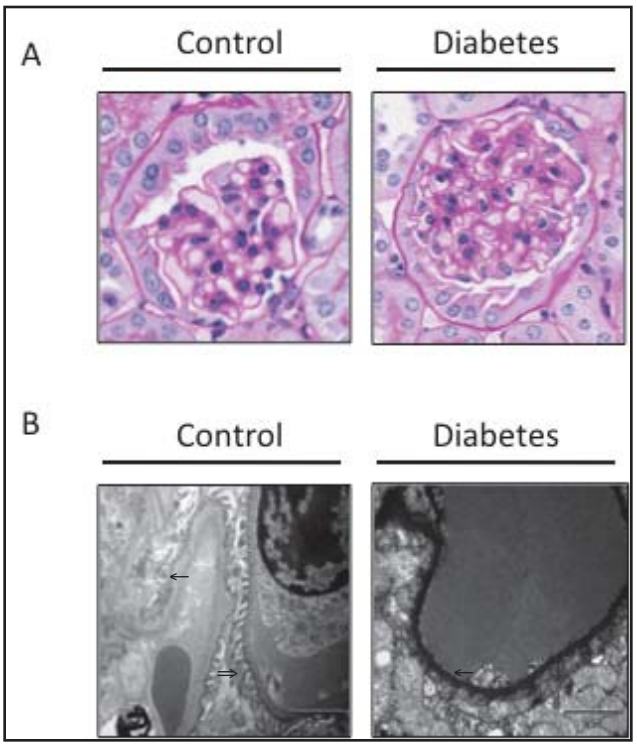

Figure 1-1. Comparison of renal structures between db/db diabetic mice and normal mice. (A) Periodic acid-Schiff (PAS) stain of glomerular sections. Diabetic glomerulus shows an expanded mesangium when compared to control. (B) Electron microscopy (EM) image of podocyte foot processes (⇒) and glomerular basement membrane (→). Loss of podocytes and GBM thickening can be seen in diabetic mice.

GBM width thickening represents one of the first structural defects, which can be detected as early as 1.5 to 2.5 years after the onset of type 1 diabetes [5]. This is followed by a progressive increase in the proportion of the glomerulus occupied by mesangial matrix and cells [9]. The mesangium is important for structural support of the glomerulus. In some cases of late-stage DN, progressive mesangial expansion leads to nodular lesions (Kimmelstiel–Wilson nodules) characterized by increased deposition of mesangial matrix and compressed glomerular capillaries [5]. Glomerulosclerosis leads to the collapse of the glomerulus and destruction of capillary lumen, resulting in loss of renal filtration [9]. Podocytes are highly specialized epithelial cells surrounding

glomerular capillaries, and their foot processes are an important component of the glomerular filtration barrier (GFB) [10]. In DN, hyperglycemia induces podocyte apoptosis [11] and foot process effacement [12], both contributing to a loss of GFB integrity. Tubulointerstitial fibrosis represents a final common outcome of ESRD, including DN [7]. Some key characteristics include deposition of ECM in the interstitium, infiltration of inflammatory cells, and tubular epithelial-to-mesenchymal transition (EMT) [7, 13].

These diabetes-induced structural defects correlate with clinically relevant functional abnormalities. Early GFB injury allows proteins normally too large to permeate the GFB to enter the glomerular filtrate, resulting in proteinuria. Microalbuminuria is the earliest clinical indicator of DN and is widely used as a predictor of future renal outcomes [13]. If left untreated, microalbuminuria can progress to overt proteinuria, ultimately leading to renal insufficiency [14]. In fact, proteinuria may also be a contributing factor to tubular injury, promoting apoptosis [15] and inflammation [16]. In the early stages of diabetes, hyperfiltration is observed due to hemodynamic changes induced by angiotensin II signaling [17]. Progressive DN eventually leads to a decline in glomerular filtration rate (GFR), reflective of mesangial expansion and glomerular lesions obliterating capillaries necessary for filtration [9].

Proper glycemic control continues to be the first line of therapy for DN [18]. However, there have been tremendous efforts in the development of drugs to further slow down or halt the progression of DN. Inhibitors of the renin-angiotensin system (RAS), particularly angiotensin converting enzyme (ACE) inhibitors or angiotensin II receptor blockers (ARBs), are currently prescribed as medications for patients with evidence of

DN. In hypertensive patients with nephropathy due to type 2 diabetes, treatment with the ARB, irbesartan was associated with a 23% decrease in relative risk for ESRD when compared to the placebo group [19]. However, a 5-year longitudinal study in normotensive type 1 diabetic patients with normoalbuminuria revealed inconsistent results. Treatment of these patients with the ACE inhibitor, enalapril, or ARB, losartan were ineffective at slowing down the progression of nephropathy, indicating additional mechanisms in the early development of DN other than the RAS [20]. In addition, recent developments of direct renin inhibitors (DRIs) show promise, as these would block the rate-limiting step of the RAS [13]. Although DRIs are currently not approved for the treatment of DN, Parving *et al.* demonstrated that the DRI aliskiren had an additive benefit when co-administered with losartan in reducing albuminuria [21]. Other classes of drugs such as statins, anti-fibrotic agents and protein kinase C (PKC) inhibitors are currently under clinical trials investigating their potential in DN treatment [13].

1.02 Molecular pathways

A vast body of research has been dedicated to the elucidation of molecular mechanisms underlying the progression of nephropathy due to diabetes. From these studies, potential therapeutic targets can be identified and ultimately serve as a basis for drug development. While there are many molecular pathways implicated in hypergylcemia and DN, below is a summary of the more recognized mechanisms, including advanced glycation end-products (AGEs), PKC, angiotensin II and TGF-β.

1.02.1 Advanced glycation end-products (AGEs)

The implication of AGEs was first demonstrated by increased immunohistochemical localization of glycation products in the glomeruli of diabetic patients [22]. AGEs are proteins modified with sugar moieties on free amino groups of lysine or arginine. The process of AGE formation can occur in both extra- and intracellular compartments, and depend directly on glucose concentration, thus associating diabetes with increased AGEs [23]. Oxidative stress also plays a role in the production of AGEs, as oxidized intermediates of glucose (glyoxal, methylglyoxal and 3-deoxyglucosone) are unstable and react readily with proteins. AGEs induce cellular damage in one of three general mechanisms: glycation of intracellular proteins alters their function, glycation of ECM proteins affect cell-matrix and matrix-matrix interactions and AGEs can affect cellular signaling through receptor for AGEs (RAGEs) [24].

The significance of AGEs in diabetic kidney disease has been investigated in a number of cell culture and animal studies. Renal expression of RAGEs is demonstrated in cell types critical for DN, including mesangial cells, podocytes and tubular cells [23]. In cultured mesangial cells, AGEs treatment induced fibronectin and collagen IV production mediated by connective tissue growth factor (CTGF) and transforming growth factor-β (TGF-β) signaling [25]. In addition, various immunochemically distinct types of AGEs promote monocyte chemoattractant protein-1 (MCP-1) secretion, thereby augmenting inflammatory processes [26]. The unfavourable effects of AGEs are directly observed in podocytes, as exposure to AGE-modified bovine serum albumin (BSA) increased apoptosis when compared to unmodified BSA treatment [27]. This effect was abrogated by RAGE-specific siRNA, specifically showing the significance of AGE-RAGE signaling in mediating podocyte apoptosis. In the same study, podocytes cultured on

AGE-modified collagen IV showed more detachment and apoptosis when compared to native collagen. Using cultured human podocytes, Doublier *et al*. demonstrated that glycated albumin downregulates the expression of nephrin, a critical protein of the slit diaphragm, and that this effect was blocked by neutralizing anti-RAGE antibodies [28]. In renal tubular cells, RAGE activation induces EMT mediated by TGF-β, resulting in a profibrotic phenotype associated with tubulointerstitial injury [29]. Recent data indicate AGE-RAGE activation also leads to CTGF synthesis in a TGF-β-independent manner [30], and CTGF is another critical mediator of tubular EMT [31]. In an experimental control rat model, continuous intravenous injection of AGEs led to renal accumulation of AGEs and renal histological pathologies resembling DN [32]. In another rat model of spontaneous diabetes, OPB-9195, an inhibitor of advanced glycation, prevented the progression of diabetic glomerulosclerosis and albuminuria [33]. Unfortunately, clinical trials for OPB-9195 were unsuccessful due to a side effect of vitamin B6 deficiency, but novel classes of AGE/RAGE inhibitors for therapeutic use are currently under investigation [23].

1.02.2 Protein kinase C (PKC)

PKCs represent a serine/threonine protein kinase superfamily important in many signaling pathways and are classified into one of three subfamilies based on biochemical properties: conventional PKCs (PKC-α, -β and -γ) are sensitive to both diacylglycerol (DAG) and Ca^{2+}, novel PKCs (PKC-δ, -ε, -η, and -θ) are DAG sensitive but non-responsive to Ca^{2+}, and atypical PKCs (PKC-λ and -ζ) are neither DAG- nor Ca^{2+}-sensitive [34]. In the diabetic kidney, high intracellular glucose activates PKC by

increased *de novo* synthesis of DAG from glycolytic intermediates [24]. Hyperglycemia also indirectly activates PKC through autocrine and paracrine actions of upregulated vasoactive peptides such as angiotensin II, vascular endothelial growth factor (VEGF) and endothelin-1 [34]. Importantly, this represents a route for Src activation induced by high glucose as PKC-δ has been shown to phosphorylate and activate protein tyrosine phosphatase-α (PTP-α), which subsequently activates Src by dephosphorylating the inhibitory Tyr-527 site [35].

As mentioned, PKCs exists in many isoforms and many of these are implicated in the pathogenesis of DN. In mesangial cells, high glucose exposure leads to the activation of PKC-α, -β, -δ, -ε and -ζ, as assessed by increased membrane translocation of these isozymes [36]. An early report using a non-specific PKC inhibitor and agonist revealed the dependence of PKCs in high glucose-mediated fibronectin accumulation in mesangial cells [37]. In a more recent study, specific blockade of PKC-α by Ro-32-0432 attenuated AGE-mediated ROS production and associated renal pathologies [38]. Also in mesangial cells, another group demonstrated that PKC-ζ mediates platelet derived growth factor (PDGF)-stimulated ROS generation by NADPH oxidase [39]. However, PKC-β appears to be one of the more critical isozymes implicated in diabetic kidney disease as evidenced by numerous animal studies. King and colleagues showed that treatment with the PKC-β-specific inhibitor ruboxistaurin (LY333531) normalized GFR and albuminuria in diabetic rats [40]. The same group further showed that inhibition of PKC-β prevented the expression of TGF-β, fibronectin and collagen IV in the glomeruli of diabetic rats [41]. Finally, in a mouse model of type 2 diabetes, ruboxistaurin was effective at ameliorating mesangial expansion associated with DN. Unfortunately, the efficacy of ruboxistaurin

has not yet translated into clinical use. Aside from adverse side effects, such as dyspepsia [34], a recent meta-analysis of three major clinical trials revealed that ruboxistaurin failed to improve renal outcomes when compared to placebo [42].

1.02.3 Angiotensin II

The RAS is a critical homeostatic hormonal cascade that is overactivated in the progression of diabetes-induced kidney disease. Classically, angiotensinogen is converted to angiotensin I by circulating or local renin. Angiotensin I is then converted to the major effector peptide angiotensin II by ACE. Angiotensin II mediates most of its effects through the angiotensin II type-1 receptor (AT_1R) [43]. Signaling through AT_1R, a G-protein coupled receptor, leads to the activation of various signaling cascades involving MAPK, Akt, PKC, and non-receptor tyrosine kinases, such as Src [43, 44].

As previously mentioned, the ARB irbesartan was effective at slowing the progression of DN in hypertensive patients independent of blood pressure reduction caused by the drug [19]. This is consistent with the fact that angiotensin II is an important mediator of intracellular signaling associated with diabetic renal disease. In primary rat MCs, high glucose stimulates the increased production of angiotensinogen and subsequent angiotensin II generation [45]. Induction of angiotensin II at the cellular level indicates autocrine/paracrine signaling in MCs. Angiotensin II has been shown to stimulate the generation of superoxide and contribute to MC hypertrophy and fibrosis [46], [47]. Interestingly, Block *et al*. demonstrated that angiotensin II promotes these effects via Nox4-mediated Src and 3-phosphoinositide-dependent protein kinase-1 (PDK-1) activation [47]. Another group also demonstrated in MCs the activation of Src by

angiotensin II treatment, subsequently leading to Smad1 activation and collagen IV synthesis [44]. Finally, angiotensin II upregulates TGF-β, a key profibrotic mediator in MCs, further augmenting the accumulation of ECM proteins [48].

1.02.4 Transforming growth factor-β (TGF-β)

TGF-β represents a critical mediator of diabetes-induced nephropathy, especially for its role in fibrosis. TGF-β consists of a large family of polypeptide growth factors implicated in a wide array of cellular processes [49]. TGF-β1, the founding member of its family, signals through ligand-receptor binding to the TGF-β type II receptor (TβR-II) which leads to dimerization and trans-phosphorylation of the TGF-β type I receptor (TβR-I) monomer on serine/threonine residues. Activated TβR-I phosphroylates Smad proteins that subsequently translocate to the nucleus to activate target genes [49].

The importance of TGF-β has been demonstrated by numerous *in vitro* studies, particularly in MCs. Indeed, high glucose exposure results in both increased TGF-β production and TβR-II synthesis [50]. TGF-β receptors and downstream SMADs have been implicated in ECM accumulation in not only MCs, but also other renal cell types [51]. In one study by Mishra *et al*., the induction of collagen I synthesis by TGF-β stimulation was shown to be mediated by Src in human MCs. They proposed that TGF-β first activates PKC-δ which subsequently activates Src and extracellular signal-regulated kinase 1/2 (ERK1/2), leading to collagen I upregulation [52]. Interestingly, signal transduction by other growth factors, such as angiotensin II [48] and PDGF [53] appear to converge on TGF-β upregulation in mediating profibrotic and hypertrophic effects.

Studies in rodent models have also revealed the pathogenic role of TGF-β. Treatment of STZ-induced diabetic mice with neutralizing anti-TGF-β antibodies attenuated renal hypertrophy and ECM gene expression associated with diabetes, when compared to mice treated with control IgG antibodies [54]. In another study by the same laboratory, an antisense oligonucleotide against TGF-β was continuously infused in STZ-induced diabetic mice over a 10-day period in order to block renal TGF-β signaling [55]. Consistent with their previous findings, treatment with the antisense oligonucleotide reduced kidney hypertrophy and ECM gene expression, when compared to diabetic mice treated with TGF-β sense oligonucleotides [55]. A more recent study in *db/db* type 2 diabetic mice showed that treatment with betaglycan, a soluble TGF-β decoy receptor, reduced albuminuria and renal structural damage when compared to vehicle-treated mice [56]. Despite the therapeutic potential of TGF-β inhibition demonstrated in mice, clinical studies investigating the effects of neutralizing anti-TGF-β antibodies in human kidney disease are still in early phases [13].

1.03 Reactive Oxygen Species

1.03.1 Overview

Many of the signaling molecules described above rely on reactive oxygen species (ROS) to mediate their effects, thereby making ROS a critical secondary messenger. ROS are derived from the incomplete reduction of oxygen (O_2) and frequently represented as superoxide anions ($O_2^{\bullet -}$), hydroxyl radicals ($HO\bullet$), hydrogen peroxide

(H_2O_2) or their reaction products [57]. Under physiological conditions, ROS modulate many signaling cascades involved in proliferation, differentiation and apoptosis, and are readily generated to counteract infections in an immune response [57]. Intracellular levels of ROS are maintained at normal concentrations by endogenous antioxidants, namely enzymes that convert ROS into less reactive compounds. In the kidney, CuZn superoxide dismutase (CuZnSOD), mitochondrial manganese superoxide dismutase (MnSOD), and heme oxygenase-1 (HO-1) are major endogenous ROS scavengers and these are upregulated in response to hyperglycemia as an adaptive response [58]. However, when increasing amounts of ROS accumulate and overwhelm the intracellular antioxidant system, as in the case of DN, pathological consequences of ROS are observed.

Proteins, lipids and DNA are all intracellular targets that can be damaged by excessive amounts of ROS. Oxidation of thiol-containing amino acids, namely cysteine, lead to formation of disulfide bridges that alter protein structure and function [57]. It is through this mechanism of enzymatic redox regulation that enables ROS to modulate various signaling pathways as a secondary messenger. For example, it is well established that oxidation of active site cysteine residues in protein tyrosine phosphatases, such as SH2-containing protein tyrosine phosphatase-2 (SHP-2) [59], lead to enzyme inactivation. As discussed in Chapter 5, ROS also play a role in regulating protein tyrosine kinase activity, including Src, however the exact effect of oxidized Src is still controversial. Lipids are also targeted by ROS. Through lipid peroxidation, secondary degradation products such as hydroperoxides, endoperoxides and aldehydes directly induce damage to proteins and DNA, or act as secondary messengers in signaling

pathways relevant in many diseases [57]. Finally, ROS can directly cause DNA damage by promoting strand breaks, and oxidation of sugar and base residues. In particular, 8-hydroxydeoxyguanosine increases mutation rates and is a marker of both nuclear and mitochondrial oxidative DNA damage [60].

1.03.2 Sources of ROS

As previously described, basal levels of intracellular ROS are important for normal physiological processes. Excessive generation of ROS that overwhelm endogenous antioxidant systems can become pathogenic by directly damaging biological macromolecules and/or altering signaling pathways as a secondary messenger. As such, it is necessary to discuss the two major sources of ROS as they relate to diabetes and the kidney: mitochondria and NADPH oxidase.

1.03.2.1 Mitochondria

The mitochondrion is an intracellular eukaryotic organelle capable of aerobic respiration, making it the predominant source of ATP production in the presence of oxygen. Its characteristic highly-folded, double-layered membrane allow it to generate a proton gradient necessary for oxidative phosphorylation of ADP into ATP, over a large surface area. To generate ATP, NADH and $FADH_2$ produced from glycolysis and the Kreb's cycle are used as substrates for the electron transport chain (ETC), a series of membrane-bound protein complexes on the inner mitochondrial membrane. As pairs of electrons are passed along the ETC from complex I to complex IV, protons are pumped against their concentration gradient into the intermembrane space, generating a proton

motive force or mitochondrial membrane potential ($\Delta\mu_{H+}$) (Figure 1-2). ATP synthase subsequently uses this membrane potential energy for oxidative phosphorylation [61].

However, the ETC is an elaborate, multi-step biological process and is not always efficient. Electron pairs that are not passed to complex IV for complete reduction of O_2 into H_2O may reduce O_2 into superoxide at serveral sites within the ETC (Figure 1-2). By analysis of various tissue types in a rat model, an estimated 0.1% of oxygen consumption under physiological conditions result in the formation of ROS from the ETC [62]. Complex I and complex III have been associated with the generation of superoxide by the single-electron reduction of O_2. Indeed, inhibitors of complex I or III, such as rotenone and myxothiazol respectively, prevent the formation of superoxide anions [61].

The mechanism of hyperglycemia-induced overproduction of mitochondrial superoxide is primarily due to increased glucose metabolism [24]. Precisely, more electron donors (NADH and $FADH_2$) from glycolysis and Kreb's cycle enter the ETC. Consequently, greater proton pumping by ETC complexes results in a high $\Delta\mu_{H+}$. An increased $\Delta\mu_{H+}$ inhibits electron transport at complex III and promotes superoxide generation by coenzyme Q. Both overexpression of MnSOD (scavenger of mitochondrial ROS) or uncoupling protein-1 (UCP-1), which collapses the proton gradient, blocked high glucose-induced ROS overproduction [24]. Recent studies by Yu *et al.* reveal that hyperglycemia also induces MAPK-dependent mitochondrial fragmentation that may contribute to ROS generation, independent of increased input of reducing equivalents into the ETC [63, 64].

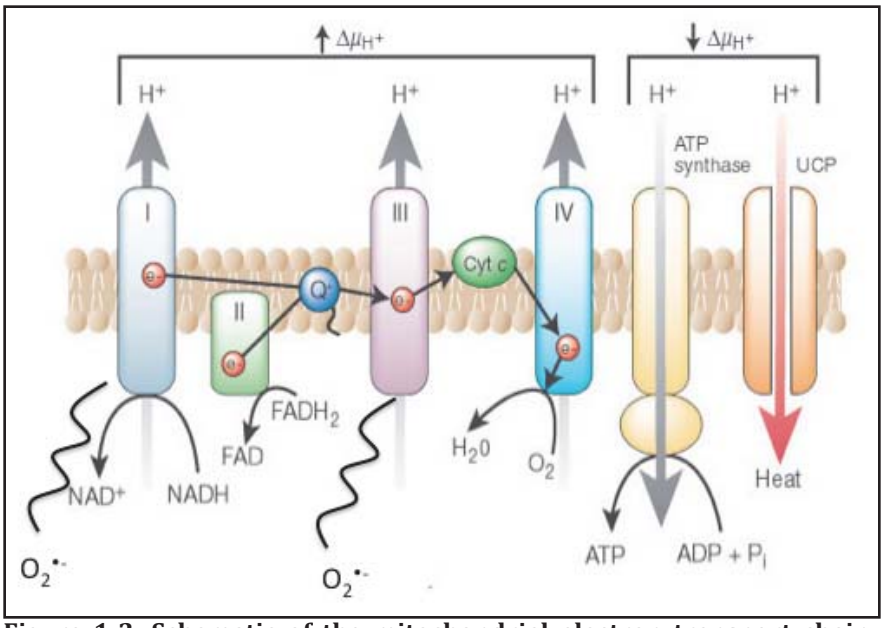

Figure 1-2. Schematic of the mitochondrial electron transport chain (ETC). Electron pairs are transferred from complex I to complex IV for the complete reduction of O2 to H2O, while pumping H+ into the intermembrane space to generate a proton gradient ($\Delta\mu_{H+}$). Incomplete reduction of O2 can occur at complex I and complex III, especially when $\Delta\mu_{H+}$ is sufficiently high. ATP synthase and uncoupling protein-1 (UCP-1) dissipates $\Delta\mu_{H+}$ by generating ATP and heat, respectively. (Adapted from Brownlee, Nature 2001)

1.03.2.2 NADPH Oxidase

The NADPH oxidase is a membrane-associated, multi-subunit protein complex originally discovered in leukocytes to play a crucial role in host defense against microorganisms. To date, seven homologues of the core NADPH oxidase enzyme, Nox, have been identified: Nox(1-5) and Duox(1-2) [65]. Essentially, these are electron carriers that utilize cytosolic NADPH as the electron donor to reduce O_2. All Nox homologues contain transmembrane alpha-helices (Figure 1-3), with heme-containing domains and a conserved C-terminal reductase domain, which also serves as a binding site for NADPH [66]. It is now evident that these Nox isoforms are expressed in many cell types and play important physiological roles outside of the immune response.

Indeed, it is now recognized as the most important mechanism for receptor-mediated ROS production [67] and that NADPH oxidases have been implicated in many diseases [65].

The prototypical NADPH oxidase originally described in phagocytic cells consists of gp91^{phox} (Nox2), p22^{phox} and additional regulatory subunits p67^{phox}, p47^{phox}, p40^{phox} and Rac-guanosine triphosphatase (Rac-GTPase) [68] (Figure 1-3). For every molecule of NADPH, Nox2 generates two superoxide anions in the extra-cytosolic space that are quickly converted to H_2O_2 and freely diffuse through biological membranes [66]. Nox2 and p22^{phox} form a membrane-bound heterodimer that requires the assembly of cytosolic regulators for full activity. p67^{phox}, also known as Nox activator-1 (NOXA1), is absolutely required for NADPH oxidase activity since it facilitates electron flow from NADPH to Nox2-bound flavin [69]. Both p47^{phox}, also known as Nox organizer-1 (NOXO1), and p40^{phox} are regulatory elements of NADPH oxidase that promote full activity by facilitating the binding of p67^{phox} to Nox2. Interestingly, p47^{phox} is activated by phosphorylation on several serine residues, which facilitates translocation to the plasma membrane for NADPH oxidase assembly [65]. Chowdhury *et al.* also demonstrated Src-dependent tyrosine phosphorylation of p47^{phox} to be important for its translocation and NADPH oxidase-derived ROS production in lung endothelial cells [70]. Finally, GTP-bound Rac is also an important regulatory component of Nox2-containing NADPH oxidase activation [71]. Its translocation occurs through an independent, yet coordinated mechanism with the translocation of other cytosolic subunits (p47^{phox} and p67^{phox}) [65]. The significance and regulation of Rac1 are discussed in detail in Chapter 1.06.

Nox4-containing NADPH oxidase has also been implicated in ROS generation, especially in the context of DN. Interestingly, the Nox4 isoform is unique in that it contains constitutive activity requiring only $p22^{phox}$ and not other regulatory subunits [71]. It is still unclear as to whether Nox4 generates superoxide or hydrogen peroxide directly. Studies have demonstrated that specific overexpression of the Nox4 isoform led to increased superoxide generation [72], [73]. However, structural comparison of Nox4 to the classical Nox2 enzyme reveals differences in an extracellular loop, supporting the claim that Nox4 generates hydrogen peroxide, rather than superoxide, directly [74].

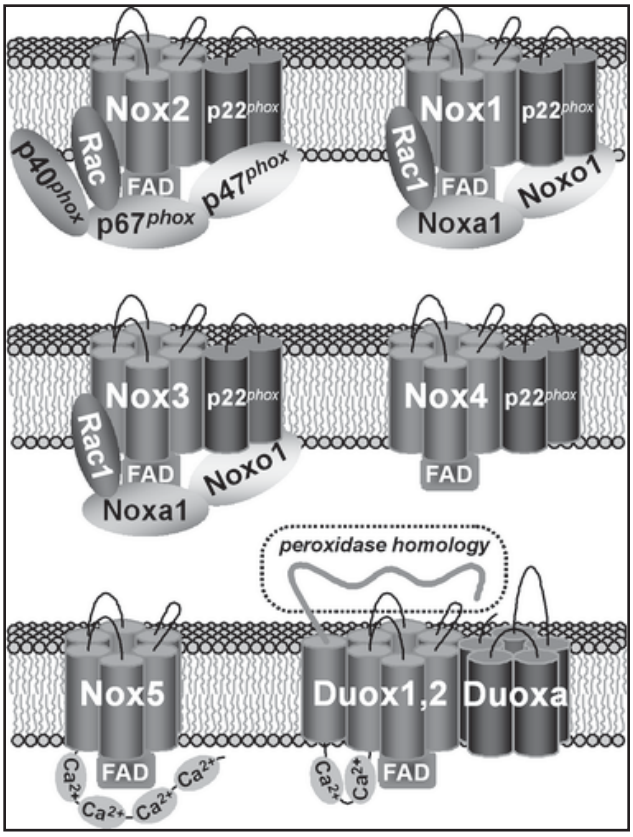

Figure 1-3. Comparison of Nox isoforms and their binding partners. The phagocytic NADPH oxidase consists of Nox2/$p22^{phox}$ heterodimer and additional regulatory subunits $p67^{phox}$, $p47^{phox}$, $p40^{phox}$ and Rac. Nox1 and Nox3 are regulated in a similar manner, where Noxa1 is equivalent to $p67^{phox}$ and Noxo1 is equivalent to $p47^{phox}$. Nox4 requires only $p22^{phox}$ as binding partner and is constitutively active. Nox5 and Duox1-2 are calcium-responsive oxidases. Duox1-2 contain extracellular peroxidase domains and forms heterodimers with Duoxa, which functions similarly to $p22^{phox}$. (Adapted from Leto *et a*l, Antioxidants & Redox Signaling 2009)

1.03.3 ROS in Diabetic Nephropathy

The role of ROS in DN is complicated; as mentioned earlier, ROS act as secondary messengers in numerous signaling pathways. Also, ROS can be derived from at least two different sources (mitochondria and NADPH oxidase) with spatial and temporal disparities and different modes of regulation. Indeed, mitochondria-derived superoxide represents a common link between hyperglycemia and several molecular pathways important in diabetic complications, including AGE formation, activation of PKCs, and the hexosamine pathway [24]. Besides the mitochondria, numerous studies from Dr. Hanna Abboud's lab indicate that Nox4-containing NADPH oxidase is critical for the progression of diabetic nephropathy in several kidney cell types ([11], [75], [76], [77]). For example, in the kidneys of STZ-induced diabetic rats, Nox4 was found to be activated and upstream of ERK1/2 and Akt, leading to hypertrophy and fibronectin expression [75]. Other isoforms of Nox, such as Nox1 and Nox2, are not as well studied in the context of DN, especially since their expression levels are not significantly altered in diabetes [78]. However, kidney glomeruli from STZ-induced diabetic rats show increased $p47^{phox}$ and $p67^{phox}$ membrane translocation and subsequent ROS production when compared to control rats [79]. Thus, this reveals a possible role of Nox1- or Nox2-containing NADPH oxidase, through activated signaling of regulator subunits rather than Nox protein induction, in mediating diabetic kidney damage.

Undoubtedly, research in both cell culture and rodent models has demonstrated a critical role of ROS in mediating nephropathy induced by diabetes. These studies brought about tremendous interest in the potential treatment of experimental models of DN with antioxidant therapy. Treatment with lithospermate B, an active antioxidant isolated from a Chinese herb, was effective at slowing the progression of nephropathy in

STZ-induced diabetic rats [80]. CuZnSOD-overexpressing transgenic mice induced with diabetes showed improved renal outcomes when compared to wild-type diabetic controls [81]. However, positive results from rodent studies have not been translated to the clinical setting. In particular, the MICRO-HOPE study failed to find any effect on nephropathy in diabetic patients treated with 400 IU vitamin E, a fat-soluble antioxidant, daily for 4.5 years [82]. In other clinical trials, Vitamin E also showed disappointing results in the prevention of cardiovascular events, but this may be explained by the lack of actual antioxidant action in human subjects as assessed by lipid peroxidation [83]. Likewise, vitamin E may not be the best agent for blocking ROS in the human kidney, especially at a low dose of 400 IU. Higher doses and in combination with other antioxidants, such as SOD or catalase mimetics, may be more effective. Novel approaches to reducing oxidative stress involve controlling free radical production and raising intracellular antioxidant defenses, and this may have a better effect than just scavenging the free radicals already present [84].

1.04 Src Kinase

1.04.1 Overview and Structure

Viral-Src (v-Src) was first discovered in the early 1900s to be constitutively active when isolated from Rous Sarcoma Virus induced chicken tumours [85]. In 1983, the cellular gene homologue, cellular-Src (c-Src), referred to here as Src, was identified and cloned [86]. It was the first proto-oncogene to be described; a gene that itself is not transforming unless mutated and/or overexpressed [87]. To date, nine members of Src

family kinases (Src, Lck, Hck, Fyn, Blk, Lyn, Fgr, Yes, and Yrk) have been discovered [87], of which Src, Fyn and Yes share the most homology and are ubiquitously expressed [88].

Src family kinases are non-receptor protein tyrosine kinases that share conserved domains in their structure, including the tyrosine kinase (SH1) domain, the Src homology 2 (SH2) domain and the Src homology 3 (SH3) domain [87] (Figure 1-4). Each family member also contains a unique, myristoylated N-terminal SH4 domain. The tyrosine kinase domain is characteristic of tyrosine and serine/threonine protein kinase folds, consisting of a small, N-terminal lobe and a large, C-terminal lobe in which the activating pTyr-416 is located [89]. It is the core catalytic region responsible for the phosphotransfer reaction, mediating transfer of a phosphate group from ATP to a target substrate. The SH2 domain functions primarily as a protein-protein recognition module and is found in diverse multidomain proteins [87]. The Src family SH2 domain is approximately 100 amino acids long with secondary structures and loops that form two recognition pockets which preferentially bind to the pYEEI motif ([89], [90]). The first pocket is highly conserved and coordinates with the phosphotyrosine motif, while the second recognizes one or more hydrophobic residues C-terminal to phosphotyrosine in a less stringent fashion, accounting for differences among SH2 domains in substrate recognition [90]. The SH3 domain, also important in protein-protein interactions, has a β-barrel structure that recognizes proline-rich sequences with a PxxP motif. Src family SH3 domains confer extra specificity by coordinating to a lysine or arginine residue either N-terminal or C-terminal to the PxxP motif [87].

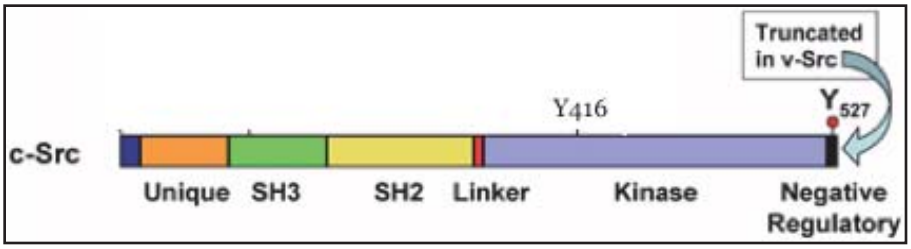

Figure 1-4. The domain structure of c-Src. The N-terminal SH4 domain is myristoylated and is unique to a specific member of Src family kinase. The SH3 and SH2 domains are important for protein-protein interactions, which bind to proline-rich and phophotyrosine motifs, respectively. The kinase domain consists of a bi-lobed structure responsible for the phosphotransfer reaction. It also contains the activating Tyr-416 residue and inhibitory C-terminal Tyr-527 residue. (Adapted from Parsons et al., Oncogene 2004)

1.04.2 Regulation

In the inactivated state, Src adopts a closed conformation whereby its SH2 and SH3 domains interact with the kinase domain on the side opposite to the catalytic cleft [87] (Figure 1-5). In particular, the SH3 domain binds to the linker sequence between the SH2 and kinase domain, while the SH2 domain binds to the C-terminal tail containing the inhibitory phosphotyrosine-527 (pTyr-527). It is important to note that these intramolecular interactions are of low affinity, since intracellular binding targets within Src do not exactly match the preferred consensus binding sequences of Src family SH2 and SH3 modules [91]. The described intramolecular interactions cause Src inactivity in several ways including displacement of the key catalytic residue Glu-310 from the active site, distortion of the activation loop which precludes substrate binding and Tyr-416 accessibility, and altering the relative orientations of the two kinase domain lobes important for optimal catalysis [87].

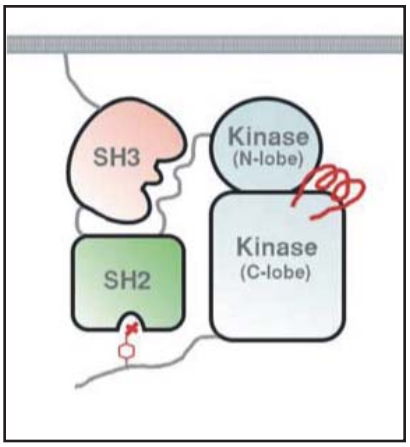

Figure 1-5. Src in its autoinhibited state. SH2/SH3 domains form intramolecular interactions with the kinase domain on the opposite side of the catalytic cleft. SH3 binds to the linker sequence between SH2 and the kinase domain, while SH2 interacts with the C-terminus via the Tyr-527 motif. (Obtained from Boggon *et a*l, Oncogene 2004)

Due to an intricate, multi-component mechanism of Src autoinhibition, there exist several routes to trigger the activation of Src kinase that ultimately lead to autophosphorylation of Tyr-416. SH2 and/or SH3-mediated binding of Src targets of higher affinity would relieve intramolecular interactions that hold Src in a 'locked', inactive state [92]. For example, PDGF receptor activation leads to Src recruitment and activation via Src SH2 domain interaction with phosphotyrosine motifs on the PDGF receptor cytoplasmic tail [93]. In addition, the phosphorylation state of Tyr-527 is tightly regulated by a number of kinases and phosphatases, as pTyr-527 is critical in SH2-mediated autoinhibition [92]. C-terminal Src kinase (Csk) is an endogenous negative regulator of Src activity as it directly phosphorylates the inhibitory Tyr-527 site [94]. In contrast, PTP-α positively regulates Src activity as it dephosphorylates Tyr-527 [95]. Thus, the regulation of Src activity is complex, involving substrate-binding competition of SH2 and/or SH3 domains, or via the actions of protein tyrosine kinases and phosphatases.

1.04.3 Src in the Kidney

There have been a number of cell culture studies documenting the involvement of Src kinase in mediating renal damage, especially via proliferative, hypertrophic and profibrotic effects in mesangial cells. Suzaki *et al*. showed that in high glucose, Src was activated and required for downstream big MAP kinase 1 (BMK1) activation, leading to increased proliferation [96]. PDGF, a potent inducer of proliferation, also activates Src in a more direct manner (as described in Chapter 1.04.2) leading to Akt and MAPK activation and subsequent induction of DNA synthesis [97]. When stimulated with angiotensin II, Nox4-derived ROS activates Src and 3-phosphoinositide-dependent protein kinase-1 (PDK-1) resulting in mesangial hypertrophy and fibronectin expression [47]. It has also been shown that TGF-β, another growth factor implicated in DN, stimulates Src activation and downstream collagen I upregulation [52]. These studies provide evidence for the importance of Src signaling in mediating the effects of high glucose and growth factors commonly associated with DN.

To date, there have been very few *in vivo* studies demonstrating the role of Src in the pathogenesis of DN. Using Western blotting and immunohistochemical staining, Mima *et al.* showed that there was increased activated pTyr-416 Src in STZ-induced diabetic rats when compared to controls. This activation was blocked when diabetic rats were treated with AT_1R blocker olmesartan, indicating that angiotensin II signals through Src, which may mediate, at least in part, the kidney pathology associated with diabetes [44]. Indeed, previous work from our laboratory demonstrating the ability of Src inhibitors to ameliorate diabetes-induced kidney pathology also provides strong evidence for the critical role of Src signaling in DN (see Chapter 2).

1.05 Vav: a Guanine Nucleotide Exchange Factor

1.05.1 Overview and Structure

Vav proteins belong to a family of DBL-homology (DH) domain-containing Rho-guanine nucleotide exchange factors (Rho-GEFs) that promote the activation of Rho-GTPases by catalyzing the dissociation of GDP from Rho in exchange for GTP [98]. Vav has been implicated in the development and function of the immune system [99], and is regarded as a proto-oncogene due to effects on cytoskeletal reorganization [100]. In mammals, three structurally related isoforms of Vav have been identified; Vav1 is expressed mainly in hematopoietic cells, while Vav2 and Vav3 are expressed in a wide distribution of cell types [99]. Vav is unique among other family members of Rho-GEFs in that it is regulated by tyrosine phosphorylation and contains both SH2 and SH3 domains [101]. Thus, Vav represents an important signaling link between tyrosine kinases and small GTPases.

Figure 1-6. The domain structure of Vav. The calponin-homology (CH) domain plays a role in maintaining Vav1/Vav3 (but not Vav2) in an inactive conformation. The acidic (Ac) region contains the important regulatory Tyr-174 (Tyr-172 for Vav2). Phosphorylation on this residue is a marker of Vav activation. The Dbl-homology (DH) domain is the region that physically interacts with Rho-GTPases for catalyzing GDP/GTP exchange, The pleckstrin-homology (PH) domain is important for membrane localization and promoting full GEF activity. The zinc finger (ZF) domain is also required for GEF activity. The proline-rich (PR) region serves as recognition sites for SH3 binding. C-terminal SH3 and SH2 domains are important for protein-protein interactions, recognizing proline-rich and phosphotyrosine motifs, respectively (Adapted from Turner *et al.*, Nature Reviews Immunology 2002)

Structurally, Vav contains multiple domains important for its regulation and function (Figure 1-6). The N-terminal calponin-homology (CH) domain appears to play a role in maintaining Vav1 and Vav3, but not Vav2, in an inactive conformation [99]. The ~50 amino acids C-terminal to the CH domain contain three regulatory tyrosine residues, Tyr-142, Tyr-160, Tyr-174, with Tyr-174 being the predominant one [102]. The characteristic DH domain is the effector structure that physically interacts with Rho-GTPases for catalysis, as point mutations of highly conserved residues in this region leads to GEF inactivity [99]. The pleckstrin-homology (PH) domain, distal to the DH domain, is involved in lipid binding, thus implicating a role in localization to membranes. Indeed, the PH domain is important for Vav activity and downstream effects, however the mechanism is unclear ([101], [103]). The zinc finger (ZF) domain also contributes to regulation of GEF activity. In vitro studies of Vav3 indicate that deletion of the PH or ZF domain abolished its GEF activity, and that the ZF region works coordinately with the PH domain for full function [104]. Finally, C-terminal SH2 and SH3 domains mediate protein-protein interactions that allow Vav to be an integral component of signaling pathways [99].

1.05.2 Regulation

The control of Vav activity is quite distinct from Src, despite both being regulated primarily by tyrosine phosphorylation and having SH2/SH3 domains. As mentioned previously, the critical and most studied phosphotyrosine residue in Vav is Tyr-174 (Tyr-172 in Vav2). In the inactivated and autoinhibited state, the conserved N-terminal regulatory tyrosine motif I/VY(174)XXL/I forms an α-helix that interacts with the DH

domain in an intramolecular manner. This binding occludes key residues in the active site of the DH domain, and prevents GTPase binding and nucleotide exchange catalysis. Upon phosphorylation, the N-terminal helix releases from the DH domain, effectively relieving autoinhibition. Phosphorylated Tyr-174 results in steric clash with active site residues Arg332 and Tyr209, causing it to be energetically unfavourable for Vav to remain in the closed, autoinhibited conformation [105]. In addition to tyrosine phosphorylation, interactions of cell membrane components with the Vav PH domain may represent an additional mode of regulation. Interestingly, the phosphatidylinositol 3-kinases (PI3K) product phosphatidylinositol-3,4,5-trisphosphate (PIP_3) enhanced phosphorylation and activation of Vav, whereas the PI3K substrate phosphatidylinositol-4,5-bisphosphate (PIP_2) was inhibitory, indicating an indirect role of PI3K on Vav activity [106].

1.05.3 Vav in the Kidney

Studies of the Vav protein have focused primarily on the immune system and cancer biology, but its importance in the kidney was demonstrated in several reports. In cultured rat MCs, Vav2 was shown to be the predominant isoform expressed and that it is activated by homocysteine stimulation leading to Rac1/NADPH oxidase activation and superoxide generation [107]. More importantly, the same group further showed the significance of Vav2 *in vivo*, and that both Vav2 and Vav3 isoforms were expressed in whole kidney sections. Using uninephrectomized Sprague-Dawley rats on a folate-free diet to induce homocysteinemia, transfection of shRNA-Vav2 plasmids via intrarenal artery injection attenuated glomerular injury and superoxide production, while

transfection of constitutively active Vav2 mimicked the effects of hyperhomocysteinemia in rats on a normal diet [108].

There have been no studies investigating the link between hyperglycemia and Vav2. Nevertheless, in a model of intrarenal hypertension, a condition associated with DN, mesangial cell RhoA activation and fibronectin overproduction was shown to be mediated by Vav2 when stimulated by mechanical stretch [109]. Strain-induced activation of RhoA also required a very rapid activation of Src-NADPH oxidase signaling upstream of Vav2 [110]. However, whether Vav2 was also necessary for mediating Src-induced activation of NADPH oxidase and ROS generation was not clear.

1.06 Rac: a small guanosine triphosphatase

1.06.1 Overview and Structure

Rho-GTPases represent a major branch of the Ras-GTPase superfamily, with Rac1, RhoA and Cdc42 being the classical and most-studied members of this subfamily [111]. Small G proteins, such as Rho-GTPases, differ from heterotrimeric G proteins in that they exist as a single, functional subunit and do not require the activity of G-protein coupled receptors for the catalysis of GDP/GTP exchange, but require GEFs instead [112]. In terms of function, all three members promote growth and inhibit apoptosis, but have distinct effects on cytoskeletal reorganization. In particular, Rac1 promotes actin polymerization and lamellipodia formation, which are curtain-like extensions forming the leading edge of migrating cells [111]. In addition, studies in phagocytes indicate that Rac represents a critical subunit for the function of Nox2-containing NADPH oxidase.

Although these studies focused on the Rac2 isoform, it has been reported that Rac1 was responsible for NADPH oxidase activation in human monocytes ([113], [114]).

In mammalian systems, three isoforms of Rac have been identified; Rac2 is exclusively expressed in hematopoetic cells while Rac1 and Rac3 have a wider expression pattern. All Rac isoforms contain a single GTPase domain followed by a polybasic sequence and a geranylgeranyl-modified cysteine [111]. This C-terminal motif plays a role in mediating membrane association of Rac [113]. Upon GTP binding and activation, Rac undergoes conformational change bringing together two regions, called switch I and switch II regions, to mediate downstream signaling. Interestingly, Rac1b represents an overactive splice variant of Rac1 with an additional 19 amino acids C-terminal to the switch II region [115]. Rac1b displays increased intrinsic GDP/GTP exchange rate, decreased autoinhibitory GTPase activity and is preferentially expressed in breast and colon cancers [113].

1.06.2 Regulation

Rac1 can be regarded as a "molecular switch", cycling between the GTP-bound, activated conformation leading to downstream effector function, and the GDP-bound inactive state. Rho-GTPases, such as Rac1, are controlled by three types of regulatory proteins: guanine nucleotide exchange factors (GEFs), GTPase-activating proteins (GAPs), and GDP-dissociation inhibitors (GDIs) [115]. As their name suggests, GEFs are positive regulators that promote the release of bound GDP in exchange for GTP. By virtue of SH2 and SH3 adapter domains, GEFs may also play a role in localizing downstream Rho-GTPase signaling to subcellular compartments, such as the plasma

membrane. GAPs, such as the family of chimaerin Rac-GAPs [116], represent negative regulators of Rho-GTPase by increasing low intrinsic activity of GTP hydrolysis, leading to the inactive GDP-bound form. GDIs are also negative regulators of Rho-GTPases by masking the C-terminal prenyl group and inhibiting interactions with GEFs and target molecules [115]. Thus, Rho-GTPase activity is tightly controlled by an intricate balance of regulatory GEFs, GAPs and GDIs.

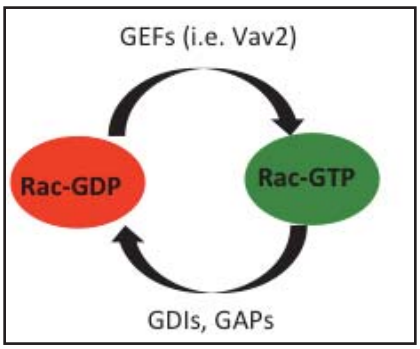

Figure 1-7. Regulation of Rac-GTPase. Guanine nucleotide exchange factors (GEFs) such as Vav2 promote the dissociation of GDP in exchange for GTP, thereby activating Rac. GTPase-activating proteins (GAPs) represent negative regulators of Rac-GTPase by increasing its low intrinsic activity of GTP hydrolysis, leading to the inactive GDP-bound form. GDP dissociation inhibitors (GDIs) form a complex with cytosolic Rac, masking the C-terminal prenyl group and inhibiting interactions with GEFs and target molecules

In phagocytes, the function of NADPH oxidase is regulated by Rac activation, in an independent but coordinated manner with other regulatory subunits ($p67^{phox}$, $p47^{phox}$, $p40^{phox}$). During NADPH oxidase activation, Rac is released from cytosolic complexes with RhoGDIs, such as RhoGDI-α, and subsequently undergo GDP to GTP exchange mediated by GEFs [115]. GTP-bound Rac directly interacts with $p67^{phox}$, the critical subunit necessary for proper electron transfer in the NADPH oxidase complex, suggesting a role of Rac as an adaptor [117]. However, recent findings indicate that Rac also directly regulates electron transfer in a two-step mechanism, and that there exists a Rac binding site conserved in Nox1, Nox2, and Nox3, but not in Nox4 or Nox5 [71]. Not

surprisingly then, Rac1 or Rac2 has been shown to be absolutely required for NADPH oxidase activity in reconstituted cell-free systems [115].

1.06.3 Rac in the Kidney

As mentioned previously, Rac2 expression is restricted to the hematopoetic system while Rac1 and Rac3 are expressed in many cell types. Of these two isoforms, Rac1 has been shown to serve a similar function as Rac2 in mediating NADPH oxidase activation. Indeed, several studies in mesangial cells have examined the role of Rac1 in oxidative stress. In a cell culture model of dyslipidemia, oxidized low density lipoproteins stimulated Rac1-dependent ROS generation leading to downstream Akt and ERK1/2 activation, resulting in MC proliferation [118]. In addition, angiotensin II also leads to very rapid Rac1/NADPH oxidase activation and downstream Akt activation, resulting in increased MC protein synthesis. Inhibition of Rac1 using a dominant-negative mutant construct was able to attenuate all downstream effects [119]. Conversely, another group showed that high glucose stimulation in MCs induced apoptosis that was downstream of Rac1-dependent ROS. Treatment with SOD, diphenyleneiodonium (DPI), or dominant-negative Rac1 construct abrogated high glucose-induced MC apoptosis [120]. Another report showed that in RhoGDI$^{-/-}$ murine mesangial cells, there was increased Rac1 activity and decreased proliferation and survival [121]. From these cell culture studies, Rac1-dependent ROS appear to mediate both proliferative and anti-proliferative effects, perhaps in response to different types of stimuli and/or different duration of exposure to ROS.

A recent publication in *Nature Medicine* reveals a novel, unexpected regulatory role of Rac1 on mineralocorticoid receptors (MRs) in the kidney [122]. Increased MR expression and signaling have been previously implicated in chronic kidney disease, such as DN. Pharmacological blockade of MR attenuates diabetes-induced renal fibrosis and upregulation of TGF-β, plasminogen activator inhibitor-1 (PAI-1), collagen I and IV, and fibronectin [123]. Shibata *et al*. reports that Rac1 positively upregulates MR-mediated transcriptional activity via p21-activated kinase (PAK) activation in podocytes. Also, they demonstrated in *Arhgdia*$^{-/-}$ mice lacking RhoGDI-α, renal Rac1 was significantly activated and this lead to renal insufficiency, including proteinuria and podocyte damage. Treatment with a pharmacological Rac-specific inhibitor blocked MR overactivity and renal damage in this model [124]. Thus, modulation of MR via PAK may represent a novel role of Rac1 in mediating renal damage in addition to ROS generation.

CHAPTER 2

RATIONALE, HYPOTHESIS AND AIMS

Chapter 2. Rationale, Hypothesis and Aims

In our previous studies of cultured rat MCs, we found that exposure to HG resulted in activation of Src, as assessed by an increase in Tyr-416 phosphorylation (Appendix Fig. 7-1A). Other groups have also reported an important function of Src in MCs, such as mediating angiotensin II- [47] and TGF-β-induced [52] matrix production. Further studies in our lab revealed that inhibition of Src with chemical inhibitors blocked HG-stimulated ERK1/2 and p38 phosphorylation and collagen synthesis. Transfection of Src-specific siRNA depleted Src and also blocked these actions of HG. *In vivo* administration of a Src inhibitor to STZ-injected diabetic mice inhibited albuminuria, mesangial matrix expansion and glomerular collagen IV and TGF-β accumulation (Data to be published). These results suggest that Src activation is a critical signaling event in the pathogenesis of DN.

Here, we further investigate Src signaling in the context of HG in primary rat MCs. As mentioned (Chapter 1.03), ROS is believed to be a critical mediator of DN. Indeed, preliminary data using chemical inhibitors in MCs suggest that Src is upstream of ROS production in the setting of HG, but the precise mechanism by which this occurs is not fully understood. **Our hypothesis** (Fig. 2-1) is that HG first activates Src, followed by Vav2 phosphorylation/activation leading to Rac1 and NADPH oxidase activation. **In addition**, Src activated by HG induces expression of Nox4, leading to ROS generation subsequent to the activation of Nox2-containing NADPH oxidase. The **specific aims** of this M.Sc. research project are:

1) To determine whether HG-induced ROS overproduction is mediated by Src

Cultured rat MCs will be exposed to normal or high glucose ± Src inhibitors or Src siRNA. ROS production will be assessed by 2'7'-dichlorofluorescein (DCF) fluorescence intensity using confocal microscopy and quantified by ImageJ software. To provide further evidence, NADPH oxidase activity assays [75] and another ROS probe, dihydroethidium (DHE), will be used to demonstrate Src-mediated ROS production.

2) To determine if Src mediates HG-induced Vav2 and Rac1 activation

To assess Vav2 activation, cultured rat MCs will be exposed to normal (5mM) or HG (25 mM) for various times and phosphorylation of Tyr-172 on Vav2 determined by immunoblotting with phospho-specific and total Vav2 antibodies. Several Src inhibitors and Src siRNA will be used concomitant with HG exposure to assess the importance of Src-mediated Vav2 activation. To assess Rac1 activity, experiments similar to those for Vav2 will be performed. However, the activation of Rac1 will be determined by cytosol-membrane fractionation followed by immunoblotting to assess Rac1 translocation [124]. To further demonstrate a Vav2-Rac1 pathway downstream of Src, the physical interaction between Src and Rac1 with Vav2 will be assessed by co-immunoprecipitation. Src inhibitors and/or Src siRNA will be used prior to HG exposure to assess the importance of Src activation in the physical association of these proteins.

3) To determine if Rac1 is required for HG-induced ROS production

Cultured rat MCs will be exposed to normal (5mM) or high glucose (25mM) ± EHT1864 (Rac1 inhibitor). ROS production will be assessed by both DCF and DHE fluorescence intensity using confocal microscopy and quantified by ImageJ software.

4) To determine if HG induces Nox4 protein expression dependent on Src

Cultured rat MCs will be exposed to NG (5mM) or HG (25mM) for various times. Src inhibitors or Src siRNA will also be used. Total Nox4 protein expression will be determined by immunoblotting with Nox4-specific antibody.

5) To elucidate the roles of Nox2 and Nox4 in HG-mediated ROS production

Cultured rat MCs will be exposed to NG (5mM) or HG (25mM) ± Nox2 siRNA, Nox4 siRNA or scrambled siRNA. ROS production will be assessed by DCF.

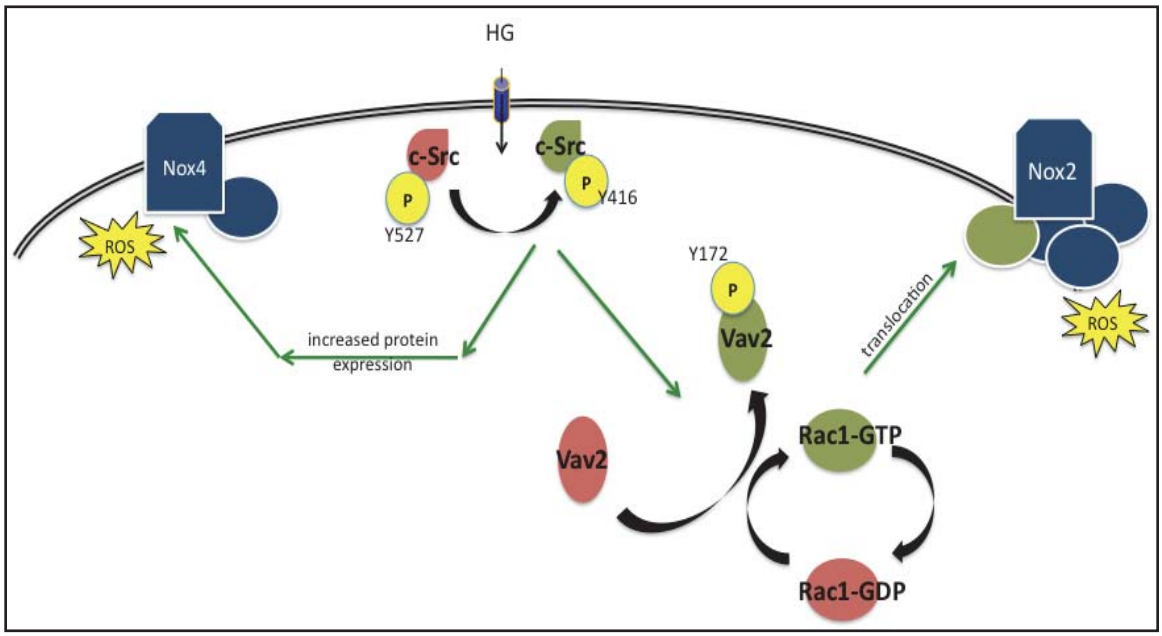

Figure 2-1. Proposed mechanism of high glucose-induced ROS production in mesangial cells. High glucose (HG) leads to Tyr-416 phosphorylation and activation of Src kinase. Activated Src phosphorylates (Tyr-172) and activates Vav2, a guanine exchange factor (GEF). Vav2 catalyzes GDP/GTP exchange of Rac1, leading to activation and translocation to the membrane. GTP-bound Rac1 is a required regulatory subunit for Nox2-containing NADPH oxidase, leading to ROS generation. In addition, Src induces expression of Nox4 following prolonged HG exposure, leading to ROS generation subsequent to the activation of Nox2-containing NADPH oxidase

CHAPTER 3

MATERIALS AND METHODS

Chapter 3. Materials and Methods

3.01 Chemicals

To inhibit the kinase activity of Src *in vitro*, various pharmacological inhibitors were used. Dasatinib (Sprycell®) was a kind gift from Bristol-Myers Squibb, AZD0530 (Saracatinib®) was purchased from Sigma, PP2, and SU6656 were purchased from Calbiochem. The rationale behind using several Src inhibitors is because of their differences in potency and selectivity. Dasatinib is a highly potent inhibitor of Src (IC_{50} = 0.0005 μM) but also has a strong effect on PDGFR (IC_{50} = 0.028 μM) [125], while SU6656 is a less potent Src inhibitor (IC_{50} = 0.28 μM) but displays minimal reactivity against PDGFR (IC_{50} > 10 μM) [126]. In most of our studies, however, the recently characterized AZD0530 was used, since it is also a potent inhibitor of Src (IC_{50} = 0.0027 μM), but displays low reactivity against PDGFR (IC_{50} > 5 μM) and EGFR (IC_{50} = 2.59 μM) [127]. By using a set of these inhibitors, in combination with Src siRNA, we are confident that Src specifically is the target implicated in our model. To inhibit Rac1 activity, the Rac1-specific inhibitor EHT1864 (Sigma) was used. For all experiments, cells were pre-treated with inhibitors one hour prior to exposure to high glucose.

3.02 Cell Culture

Primary rat mesangial cells were previously isolated from male Sprague-Dawley rat kidney glomeruli from the laboratory of Dr. Catharine Whiteside (University of

Toronto), as previously described [36]. Cells were thawed from liquid nitrogen and propagated, and passages 8 to 20 were used in experiments. Mesangial cells were grown on 10-cm culture dishes or on glass coverslips in 6-well plates in Dulbecco's Modified Eagle's Medium (DMEM; Sigma-Aldrich) containing 5.6 mM D-glucose (Sigma-Aldrich), 20 mM 4-(2-hydroxyethyl)-1-piperazineethanesulfonic acid (HEPES; Sigma-Aldrich), 5% fetal bovine serum (FBS, Thermo Scientific), 100U penicillin (Invitrogen Life Technologies) and 100 μg streptomycin (Invitrogen Life Technologies). At 70-80% confluency, cells were growth-arrested in 0.5% FBS for 48 h containing either 5.6 mM or 25 mM glucose. In some experiments, cells were pretreated with the inhibitors dasatinib (100 nM), AZD0530 (50 nM), PP2 (2 μM), SU6656 (2.5 μM), or EHT1864 (2 μM).

3.03 siRNA Transfection

To knockdown cellular mRNA and protein levels of Src, Nox2 and Nox4, cells were forward transfected using either Lipofectamine RNAiMAX reagent (Invitrogen Life Technologies) or INTERFERin transfection reagent (Polyplus Transfection). Src-, Nox2- and Nox4-specific Stealth RNAi siRNAs and scrambled siRNA were purchased from Invitrogen Life Technologies. For 6-well plates, 1-5 nM of Src siRNA, 20 nM of Nox2 siRNA, 20 nM of Nox4 siRNA or 5 nM of scrambled siRNA were mixed in 100 μl/well of Opti-MEM Medium (Invitrogen Life Technologies). For some experiments, 8 μl/well of INTERFERin transfection reagent were added directly into the siRNA mixture, vortexed and incubated for 10 min at room temperature. 100 μl of final transfection mix was added to each well containing 2 ml of 20% FBS DMEM with no antibiotics. For other experiments, 2.5 μl/well of Lipofectamine RNAiMAX reagent was mixed with 100

μl/well of Opti-MEM Medium. The siRNA mixture and transfection reagent mixture were incubated for 5 min at room temperature separately. 100μl/well of each mixture were combined and incubated for an additional 20 min. 200μl of final transfection mix was added to each well containing 2ml of 20% FBS DMEM with no antibiotics. After 24 h, cells were growth-arrested in 1% FBS DMEM for an additional 48 h. For 10-cm dishes, an identical protocol was used with 5 times the reagent volumes as described for 6-well plates.

3.04 DCF Fluorescence

To evaluate intracellular ROS, chloromethyl-2',7'-dichlorodihydrofluorescein diacetate (CM-H_2DCFDA; Santa Cruz) was used as a probe. CM-H_2DCFDA is a lipid-soluble, membrane permeable compound that is cleaved by intracellular esterases to form the membrane-impermeable CM-H_2DCF intermediate. This enzymatic reaction enables cells to retain the dye more readily, whereby intracellular ROS react with CM-H_2DCF to form the fluorescent product [128]. In brief, cells cultured on glass coverslips were washed once with warm phosphate buffered saline (PBS; 2.7 mM KCl, 1.4 mM KH_2PO_4, 137 mM NaCl, 8 mM Na_2HPO_4) and incubated in DMEM containing 1 μM of CM-H_2DCFDA for 30 min at 37^{o}C. Cells were then washed three times with warm PBS and incubated in PBS for the duration of the experiment. Intracellular ROS production, as assessed by fluorescence intensity, was observed by confocal laser scanning microscopy (Zeiss) using an excitation wavelength of 488 nm and an emission wavelength of 513 nm. For each experimental condition, fluorescence intensity per cell was analyzed using ImageJ software (NIH) using 60-90 cells from three independent experiments.

3.05 DHE Fluorescence

To supplement the DCF data, dihydroethidium (DHE; Invitrogen) was used as another ROS probe in similar experiments. DHE reacts with superoxide to generate the specific, fluorescent product 2-hydroxyethidium [129]. However, recent studies showed that DHE can also react with general ROS, i.e. ROS, to form the less specific product ethidium [130]. DHE was used here to investigate overall intracellular ROS production. In brief, cells cultured on glass coverslips were washed once with warm PBS and incubated in DMEM containing 1 μM of DHE for 30 min at 37^{o}C. Cells were then washed three times with warm PBS and incubated in PBS for the duration of the experiment. Intracellular ROS production, as assessed by fluorescence intensity, was observed by confocal laser scanning microscopy (Zeiss) using an excitation wavelength of 488 nm and an emission wavelength of 588 nm. For each experimental condition, fluorescence intensity per cell was analyzed using ImageJ software (NIH) using 60-90 cells from three independent experiments.

3.06 NADPH Oxidase Activity Assay

To assess the activity of NADPH oxidase, a lucigenin-based chemiluminescence method which measures superoxide generation was performed as described with minor modifications [75] Briefly, mesangial cells were washed twice with ice-cold PBS and were scraped from the dish in lysis buffer containing 20 mM KH_2PO_4, pH 7.0, 1 mM EGTA and a complete protease inhibitor cocktail (Roche). Cell suspensions were homogenized by passing them through a 26.5-gauge needle 10 times on ice, and aliquots

of the homogenates were used immediately. To start the assay, 100 µl of homogenate were added into 900 µl of assay buffer containing 50 mM KH_2PO_4, pH 7.0, 1 mM EGTA, 150 mM sucrose, 5 µM lucigenin, 100 µM NADPH and a protease inhibitor cocktail. Photon emission in terms of relative light units (RLUs) was measured every 30 seconds in a GloMax 20/20 luminometer (Promega) A background measurement containing homogenates but no NADPH representing non-specific units was subtracted from each reading to determine specific activity. NADPH oxidase activity was expressed as fold change versus untreated samples, in RLUs per milligram of protein. Protein content was measured using the Bio-Rad protein assay.

3.07 Co-immunoprecipitation

A co-immunoprecipitation approach was used in order to assess intracellular protein-protein interactions. Mesangial cells were washed twice with ice-cold PBS and were scraped from the dish in lysis buffer containing 50 mM Tris, pH 7.4, 120 mM NaCl, 1% NP-40, 1 mM NaF, 2 mM Na_3VO_4, 20 mM $Na_4P_2O_7$, 5 mM β-glycerophosphate and a complete protease inhibitor cocktail (Roche). Cell suspensions were homogenized by passing them through a 26.5-gauge needle 10 times on ice. Protein content was measured using the Bio-Rad protein assay. 750-1000 µg of protein was mixed with 2 µg of polyclonal anti-Vav2 antibody (Santa Cruz) in 750 µl of lysis buffer and incubated overnight at 4^{o}C with rotation. 40 µg of Protein A Sepharose (GE Healthcare) was added to the immunoprecipitation mixture and incubated for an additional 2 h at 4^{o}C with rotation. Following incubation, the samples were centrifuged at 10,000 g for 30 sec at 4^{o}C. The supernatant was discarded and the beads were washed three times with wash

buffer (20 mM Tris, pH 8.0, 120 mM NaCl, 1 mM EDTA, 0.5% NP-40). After the last wash, wash buffer was removed entirely by aspiration with a 21.5-gauge needle. The samples were eluted from pellets in 50 µl of 4X sample buffer (260 mM Tris, pH 6.8, 40% glycerol, 8% sodium dodecyl sulfate (SDS), 0.04% bromophenol blue, 10% 2-mercaptoethanol) and 130 µl of lysis buffer. Samples were vortexed, boiled for 5 min and centrifuged at 10 000 rpm for 30 sec at room temperature. 50 µg of eluted proteins were separated by SDS-PAGE, transferred to a nitrocellulose membrane and visualized by Western blot analysis.

3.08 Cytosol-membrane Fractionation

In order to assess Rac1 activity, relative membrane content of Rac1 protein in mesangial cells was determined using an ultracentrifugation protocol to isolate cytosol and membrane fractions [124]. Cells were washed twice with ice-cold PBS and were scraped from the dish in detergent-free lysis buffer containing 50 mM Tris, pH 7.5, 10 mM EGTA, 2 mM EDTA, 1 mM $NaHCO_3$, 5 mM $MgCl_2 \bullet 6H_2O$, 1 mM NaF, 2 mM Na_3VO_4, 20 mM $Na_4P_2O_7$, 5 mM β-glycerophosphate and a complete protease inhibitor cocktail (Roche). Cell suspensions were homogenized by passing them through a 26.5-gauge needle 10 times on ice and ultracentrifuged at 100,000 g for 1 h at 4^oC. The resulting supernatant was transferred to a new eppendorf tube and designated the cytosolic fraction. The pellet was resuspended in lysis buffer (as above) containing 1% Triton-X by first passing samples through a 21.5-gauge needle 10 times, followed by a 26.5-gauge needle 10 times on ice. Samples were centrifuged at 16,000 g for 30 min at 4^oC. The resulting supernatant was transferred to a new eppendorf tube and designated

the membrane fraction. Protein content was measured using the Bio-Rad protein assay and equal amounts of protein from cytosol and membrane samples were separated by SDS-PAGE, transferred to a nitrocellulose membrane and visualized by Western analysis. Rac1 was immunoblotted to assess membrane and cytosol content of Rac1 protein and Na^+/K^+ ATPase was immunoblotted to assess membrane purity.

3.09 Western Blotting

Mesangial cells were washed twice with ice-cold PBS and were scraped from the dish in lysis buffer containing 10 mM Tris, pH 7.4, 100 mM NaCl, 1 mM EDTA, 1 mM EGTA, 1% Triton-X, 0.5% sodium deoxycholate, 0.1% SDS, 1 mM NaF, 2 mM Na_3VO_4, 20 mM $Na_4P_2O_7$, 5 mM β-glycerophosphate and a complete protease inhibitor cocktail (Roche). Cell suspensions were homogenized by passing them through a 26.5-gauge needle 10 times on ice. Protein content was measured using the Bio-Rad protein assay. Samples were mixed with 4X sample buffer in a 3:1 ratio. For immunoblotting, equal amounts of protein were separated by SDS-PAGE (7.5%-12.5%), transferred to nitrocellulose, and immunoblotted with the following antibodies: anti-pVav2 (1:1000), anti-Vav2 (1:1000), anti-Rac1 (1:1000), anti-Na^+/K^+ ATPase α-subunit (1:1000), anti-Src (1:1000), anti-gp91-phox (Nox2) (1:1000), anti-Nox4 (1:1000), and anti-β-actin (1:5000). Immunocomplexes were visualized by an enhanced chemiluminescence detection kit (KPL, Inc.) using horseradish peroxidase-conjugated anti-rabbit (Bio-Rad) or anti-mouse (The Jackson Laboratory) secondary antibodies. Antibodies against pVav2, Vav2, Na^+/K^+ ATPase, and β-actin were purchased from Santa Cruz Biotechnology. Antibodies against Rac1 and gp91-phox were purchased from Millipore. Antibody against Src was

purchased from Cell Signaling. Antibody against Nox4 was purchased from Novus Biologicals.

3.10 Statistical Analysis

Quantitative results are expressed as mean ± standard error (SE). Statistical analyses were performed with GraphPad Prism 4.0. Unpaired Student *t*-tests were used to compare the means of two groups. One-way analysis of variance (ANOVA) was applied to compare the means of three or more groups, followed by Neuman-Keuls post-hoc analysis. $P < 0.05$ was considered to be significant.

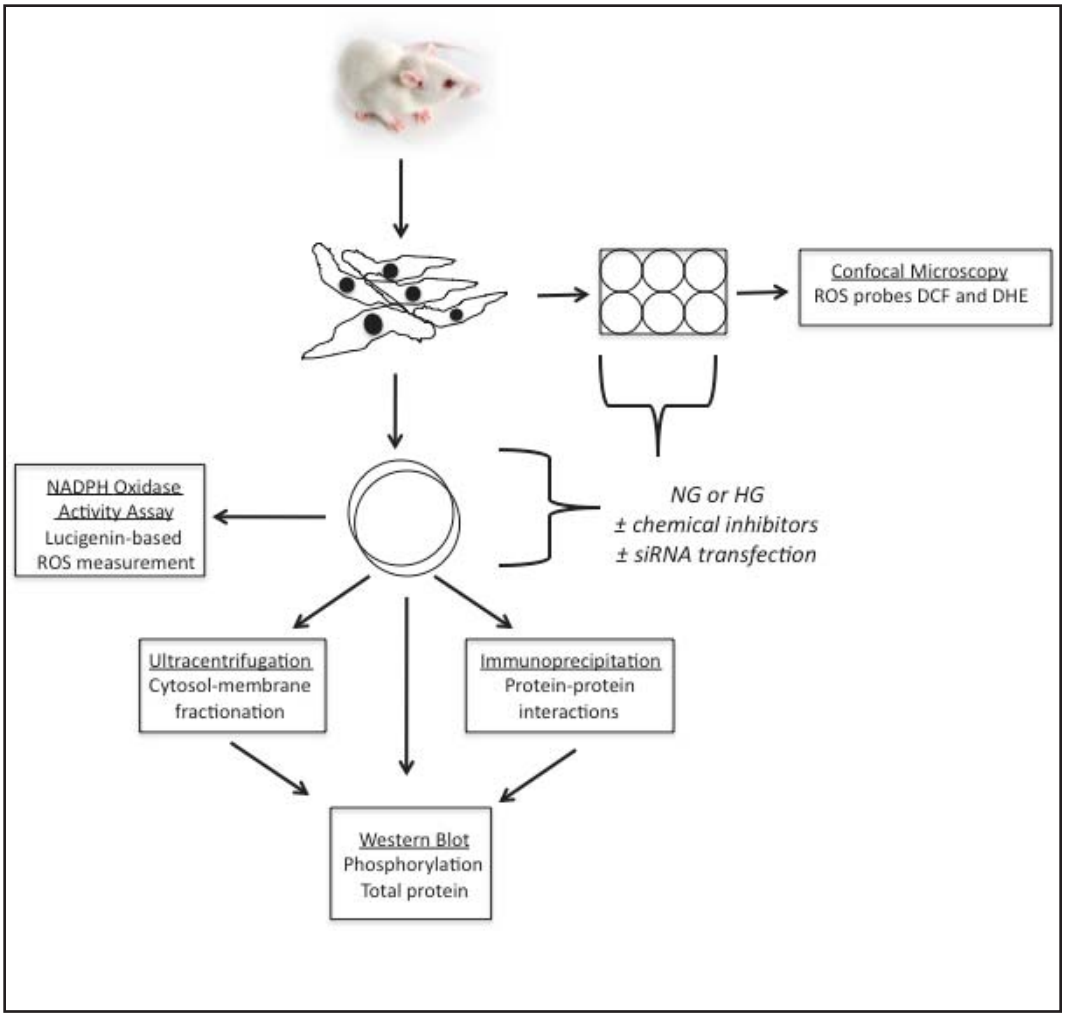

Figure 3-1. Simplified schematic of experimental approach. See text for more details. Primary rat mesangial cells (MCs) were previously isolated and cultured in 10-cm dishes or coverslips in 6-well plates. DCF and DHE were used to assess ROS generation by confocal microscopy. Also, NADPH oxidase activity was assayed in cellular lysates. Western blots were used to assess the phosphorylation state of Vav2 and total protein levels of other targets. Prior to Western blotting in some experiments, cellular lysates were ultracentrifuged to separate cytosol and membrane fractions in order to evaluate Rac1 activation, or immunoprecipitated to assess physical interactions between Vav2 and Src, as well as Vav2 and Rac1. (Photo of Sprague-Dawley rat obtained from www.criver.com)

CHAPTER 4

RESULTS

Chapter 4. Results

4.01 Src is required for HG-induced ROS production

In previous studies in cultured rat MCs, we demonstrated a critical role of Src in HG-stimulated collagen synthesis (unpublished). It is also well established that ROS contributes to the progression of DN (see Chapter 1.03). Since Src is known to activate NADPH oxidase in some cells [131], but has also been found to be activated in response to ROS, we sought to investigate whether HG leads to Src-dependent ROS generation in MCs by three methods: DCF fluorescence, DHE fluorescence, and the NADPH oxidase activity assay. To assess whether Src is important in HG-induced ROS production, DCF fluorescence was used to detect intracellular ROS levels. In HG (25 mM), ROS production was increased when compared to NG (5 mM), and this effect was attenuated in the presence of several Src inhibitors, Dasatinib (100 nM), PP2 (2 μM), SU6656 (2.5 μM) or AZD0530 (50 nM) (Fig. 4-1A). The dose response of Dasatinib and AZD0530 were determined (Appendix Fig. 7-1), while PP2 and SU6656 dosages were based on previous studies [96, 109]. Similarly, transfection with Src siRNA was used to specifically knockdown intracellular levels of Src (Appendix Fig. 7-2). Src-specific siRNA decreased ROS production induced by HG at 3 h and 24 h (Fig. 4-1B). Experiments using another ROS probe DHE also revealed that 3 h of HG exposure increased ROS production, and this effect was blocked by Dasatinib and AZD0530 (Fig. 4-1C). We then assessed ROS generation using an NADPH oxidase activity assay to provide further evidence. This assay detects superoxide generation in the presence of

exogenously added NADPH, thus preferentially assessing NADPH oxidase activity [132]. At 3 h and 12 h of HG exposure, there was an increase in NADPH oxidase activity when compared to NG (Fig. 4-1D). Treatment with AZD0530 attenuated the HG-induced increase in NADPH oxidase activity (Fig. 4-1E). Taken together, these results indicate that Src is required for ROS overproduction in response to HG.

A

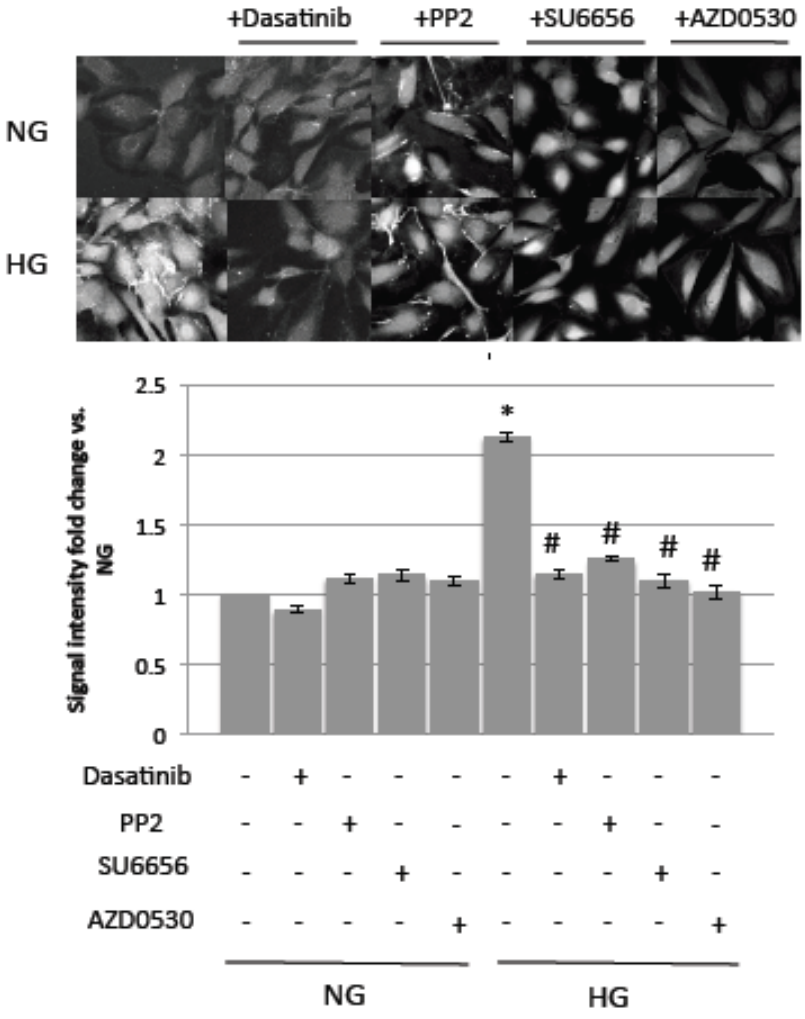

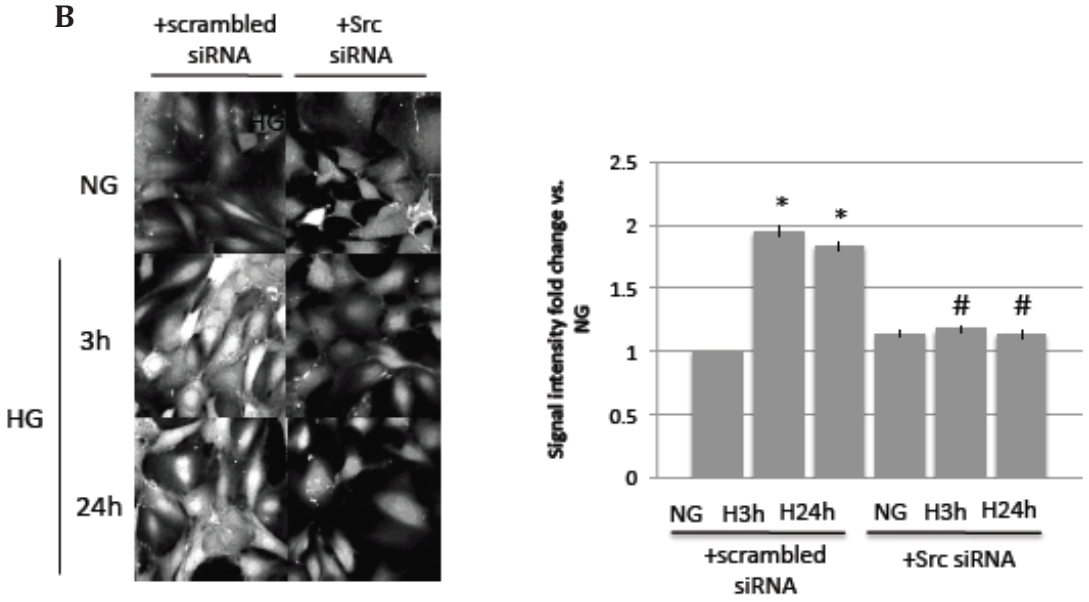
B
+scrambled siRNA
+Src siRNA
NG
HG
3h
24h
HG
Signal intensity fold change vs. NG
2.5
2
1.5
1
0.5
0
*
*
#
#
NG H3h H24h
NG H3h H24h
+scrambled siRNA
+Src siRNA

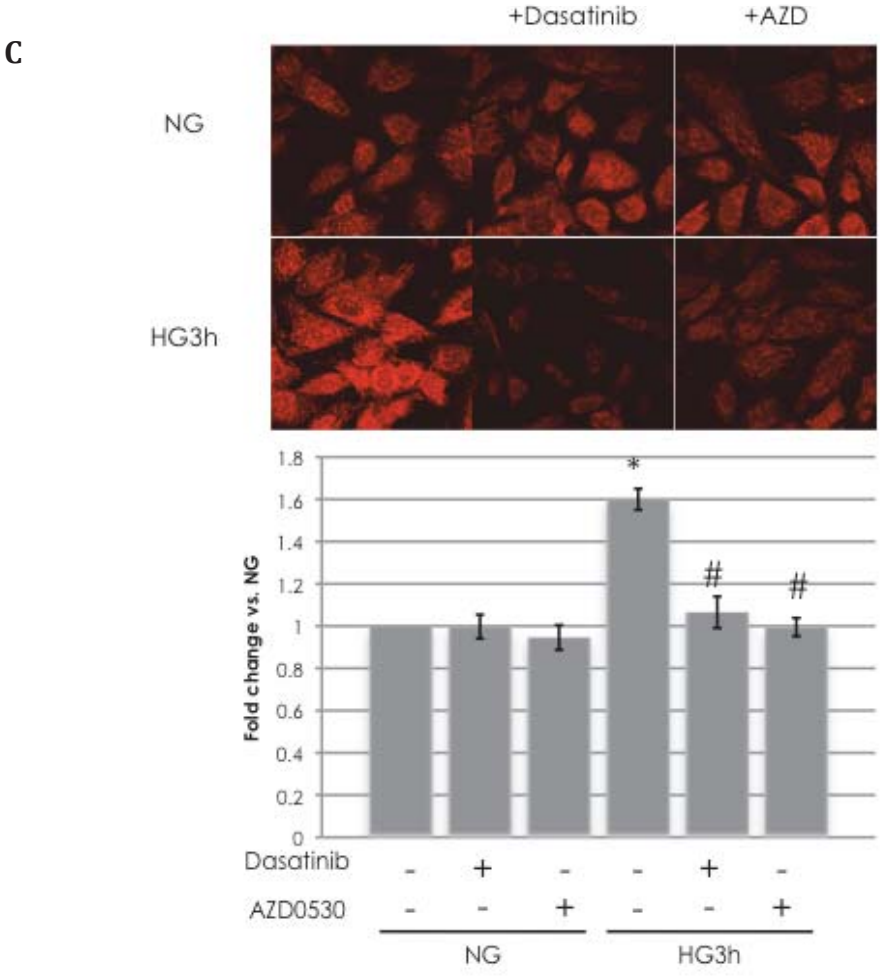
C
+Dasatinib
+AZD
NG
HG3h
Fold change vs. NG
1.8
1.6
1.4
1.2
1
0.8
0.6
0.4
0.2
0
*
#
#
Dasatinib - + - - + -
AZD0530 - - + - - +
NG
HG3h

D

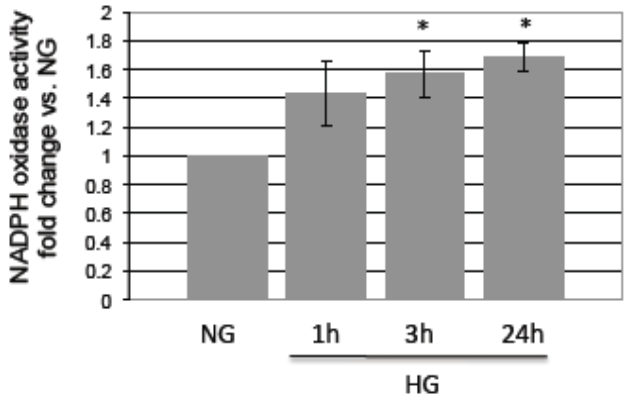

E

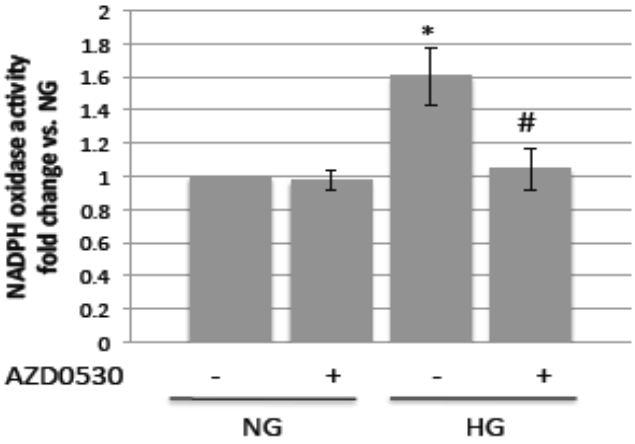

Figure 4-1. HG stimulates Src-dependent ROS production. Primary rat mesangial cells were serum starved for 48h prior to experiments. Cells were incubated in normal glucose (NG; 5mM) or high glucose (HG; 25mM). (A) ROS production in 3h HG assessed by DCF. Src inhibitors, Dasatinib (100nM), PP2 (2μM), SU6656 (2μM), or AZD0530 (50nM), were added 1h prior to HG treatment. (B) ROS production in 3h and 24h HG, assessed by DCF. Src-specific siRNA (2nM) or scrambled negative control (2nM) were added for 24h, washed and followed by 48h serum starvation. HG treatment was added during serum starvation, in the final 3 h or 24 h before experimentation. (C) ROS production in NG and 3h HG (performed as in A) assessed by DHE with or without Dasatinib or AZD0530. *Top,* Representative micrographs showing DCF or DHE fluorescence. *Bottom,* Histograms represent the average pixel intensity per cell using ImageJ analysis and data are expressed as fold change of NG. Values are the mean ± SE of 80-100 cells per group from three separate experiments. *, $p<0.01$ versus NG. #, $p<0.01$ versus HG. (D-E) NADPH oxidase activity assay. Src inhibitor AZD0530 (50nM) was added 1h prior to HG treatment. For the experiment, cells were homogenized and added to assay buffer containing 5μM lucigenin and 100 μM NADPH. Photon emission was measured as relative light units (RLU) every 30s for 5 min in a luminometer. *, $p<0.05$ versus NG. #, $p<0.05$ versus HG.

4.02 HG activates a Vav2-Rac1 pathway mediated by Src

To elucidate the molecular mechanism of Src-mediated ROS production stimulated by HG, we assessed whether Vav2-GEF and downstream Rac1-GTPase were involved. As described previously, Rac1 represents a necessary subunit for the assembly and activation of Nox1-, Nox2-, and Nox3-containing NADPH oxidase (Chapter 1.06). Indeed, Gianni *et al.* demonstrated in a colon carcinoma cell line that Src mediates a downstream Vav2-Rac1 pathway resulting in NADPH oxidase ROS production [131]. Here, we report that a similar mechanism is involved in which Src mediates HG-induced NADPH oxidase activation in MCs.

4.02.1 HG induces Vav2 Tyr phosphorylation and activation by a Src-dependent mechanism

Vav2 is a guanine nucleotide exchange factor that is activated when phosphorylated on Tyr-172 [105]. In primary cultures of rat MCs, Vav2 phosphorylation was assessed by immunoblotting total cell lysates with an anti-pVav2 (Tyr172) antibody. HG (25 mM) exposure resulted in a rapid stimulation of Vav2 phosphorylation observed within 1 h and maintained for at least 24 h compared to NG (5mM; Fig. 4-2A). Treatment with the Src-specific inhibitors, PP2, SU6656 or AZD0530 was able to attenuate the increase in Vav2 phosphorylation induced by high glucose (Fig. 4-2B and Fig. 4-2C). In addition to pharmacological inhibition, Src knockdown with Src-specific siRNA similarly decreased HG-induced Vav2 phosphorylation (Fig. 4-2D). Total Vav2 expression did not significantly change with HG. These results indicate that Src is required for the phosphorylation and activation of Vav2 in HG.

A

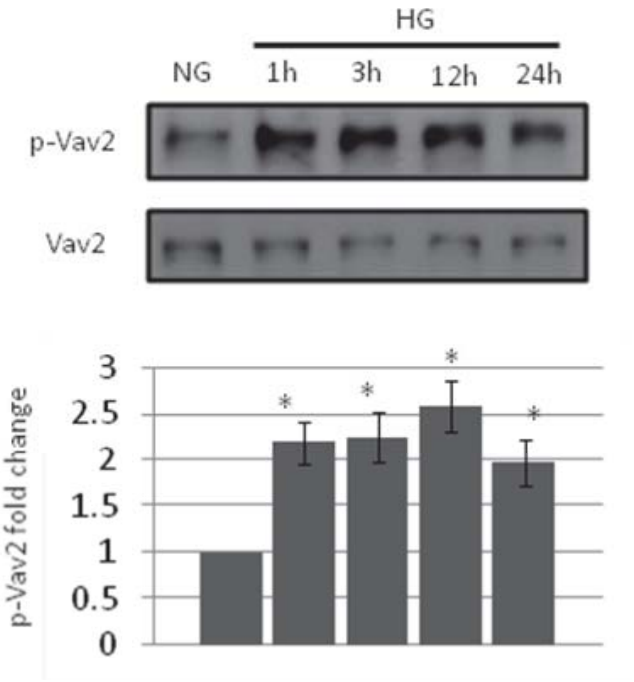
HG
NG
1h
3h
12h
24h
p-Vav2
Vav2
p-Vav2 fold change
3
2.5
2
1.5
1
0.5
0
*
*
*
*

B

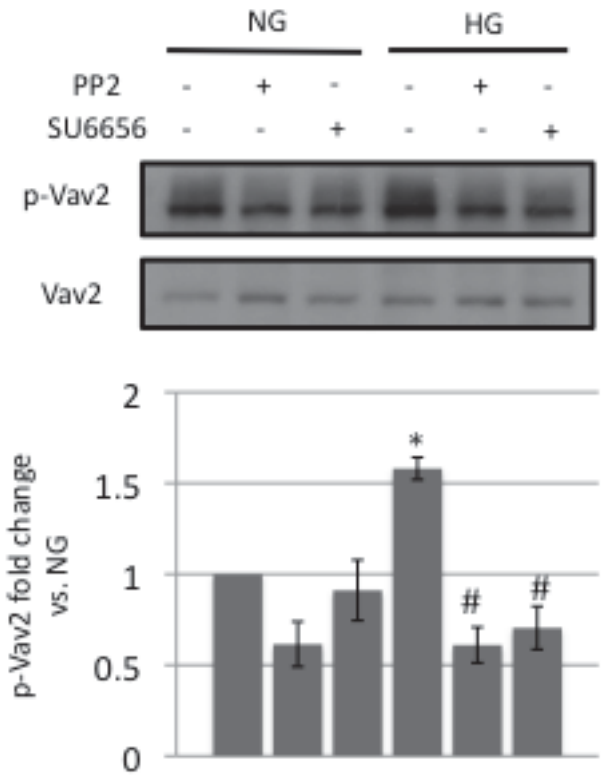
NG
HG
PP2
SU6656
p-Vav2
Vav2
p-Vav2 fold change vs. NG
2
1.5
1
0.5
0
*
#
#

C

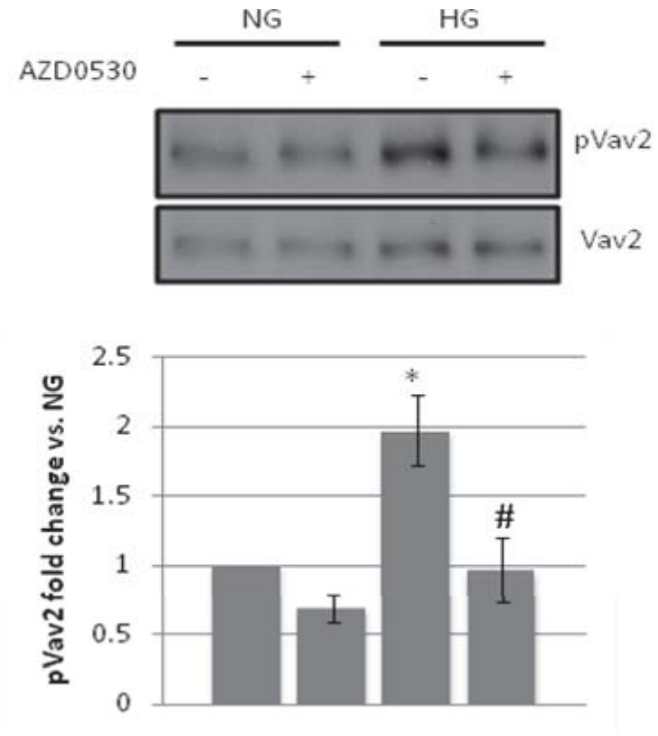
NG
HG
AZD0530
- + - +
pVav2
Vav2
pVav2 fold change vs. NG
2.5
2
1.5
1
0.5
0
*
#

D

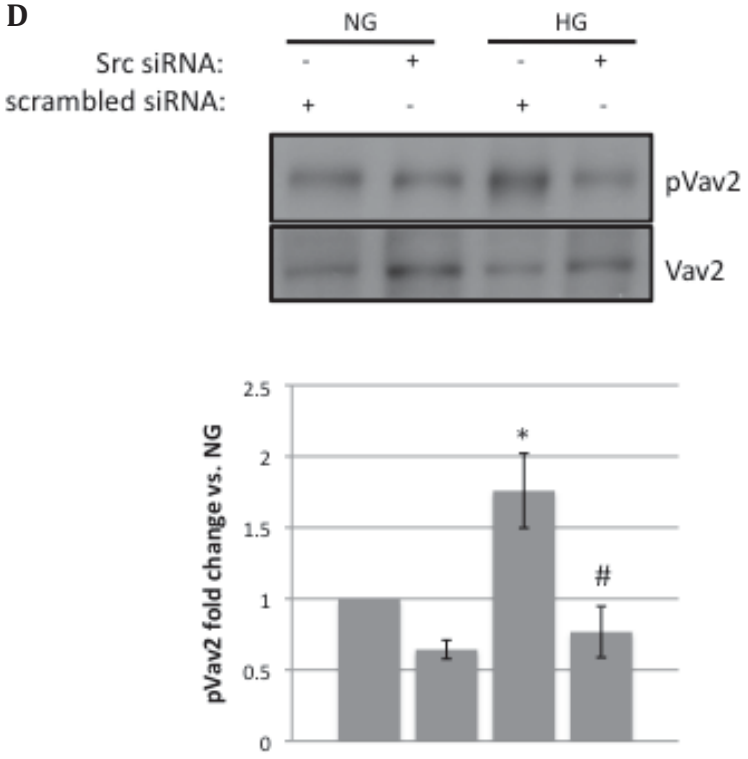
NG
HG
Src siRNA:
scrambled siRNA:
- + - +
+ - + -
pVav2
Vav2
pVav2 fold change vs. NG
2.5
2
1.5
1
0.5
0
*
#

Figure 4-2. High glucose phosphorylation of Vav2 is Src-dependent. Primary rat mesangial cells were serum starved for 48h and were incubated in normal glucose (NG; 5mM) or high glucose (HG; 25mM). Vav2 phosphorylation was determined by immunoblotting 15-20 μg of total lysates with anti-pVav2 (Tyr172) antibody. Total Vav2 expression was included as a loading control. (A) Vav2 Tyr-172 phosphorylation in HG at 1h, 3h, 12h and 24h. (B,C) Vav2 phosphorylation in 3h HG. Src inhibitors, PP2 (2μM), SU6656 (2.5μM) or AZD0530 (50nM), were added 1 h before stimulation with HG. (D) Vav2 phosphorylation in 3h HG. Src-specific siRNA (2nM) or scrambled negative control (2nM) were added for 24h, washed and followed by 48h serum starvation. *Top*, Western blot shown represents 3-4 independent experiments. *Bottom*, Histograms represent densitometry of p-Vav2 corrected to total Vav2 in each condition. The data are expressed as fold change of NG. Values are the mean ± SE of 3-4 independent experiments. *, $p<0.05$ versus NG. #, $p<0.05$ versus HG

4.02.2 HG induces Src-dependent Rac1 activation

The small GTPase Rac1 is a regulatory subunit of NADPH oxidase and translocates to the membrane when active in its GTP-bound form [68]. Here, we examined if HG affects Rac1 localization in membrane versus cytosol fractions, and whether this was dependent on Src. Membrane-cytosol fractionation was performed using ultracentrifugation of rat MC lysates as described in methods, followed by immunoblotting of Rac1. HG induced a relatively rapid (within 1 h) and persistent (at least up to 12 h) increase in Rac1 membrane localization compared to NG (Fig. 4-3A). Treatment with AZD0530 blocked this translocation effect of HG, consistent with Src being necessary for HG-induced Rac1 activation (Fig. 4-3B). Na^+/K^+ ATPase was also immunoblotted as a marker of membrane purity and showed only membrane localization. In a preliminary experiment, total Rac1 protein from whole cell lysates did not significantly change in HG or HG with AZD0530 when compared to NG (Fig. 4-3C), supporting a translocation effect of Rac1 in these conditions and not a change in total cellular content of Rac1.

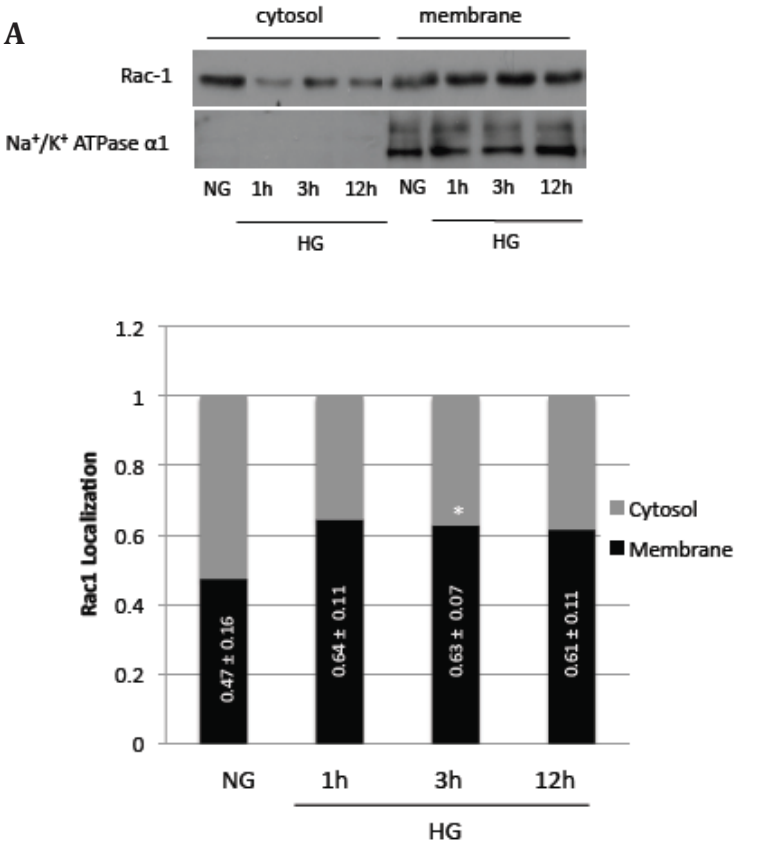
A
cytosol
membrane
Rac-1
Na+/K+ ATPase α1
NG 1h 3h 12h NG 1h 3h 12h
HG
HG
Rac1 Localization
1.2
1
0.8
0.6
0.4
0.2
0
0.47 ± 0.16
0.64 ± 0.11
0.63 ± 0.07
0.61 ± 0.11
*
Cytosol
Membrane
NG 1h 3h 12h
HG

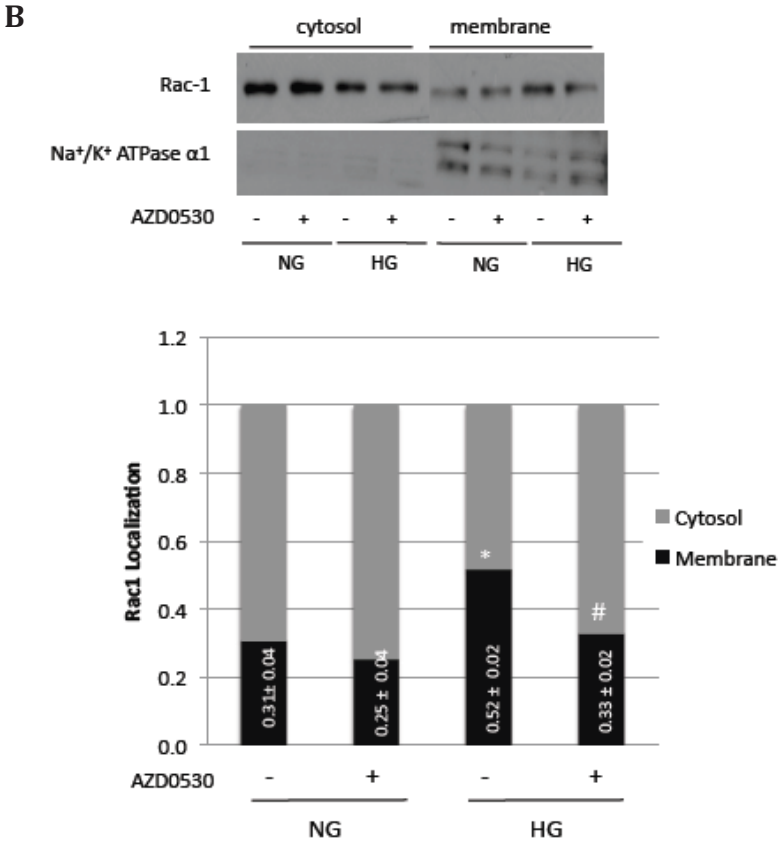
B
cytosol
membrane
Rac-1
Na+/K+ ATPase α1
AZD0530 - + - + - + - +
NG HG NG HG
Rac1 Localization
1.2
1.0
0.8
0.6
0.4
0.2
0.0
0.31± 0.04
0.25 ± 0.04
0.52 ± 0.02
0.33 ± 0.02
*
#
Cytosol
Membrane
AZD0530 - + - +
NG HG

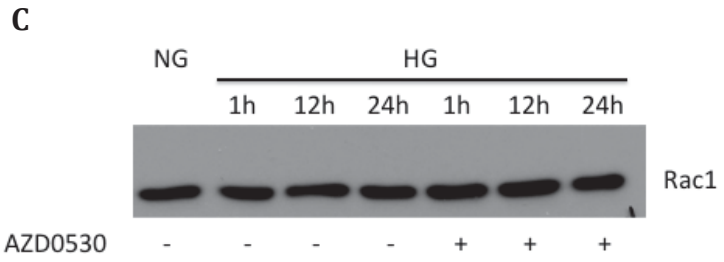

Figure 4-3. High glucose activation of Rac1 is Src-dependent. Primary rat mesangial cells were serum starved for 48 h before harvest and were incubated in normal glucose (NG; 5mM) or high glucose (HG; 25mM). After the times indicated, 0-12 h, cells were harvested and homogenized, and total lysates were separated by ultracentrifugation into cytosol and membrane fractions, followed by immunoblotting with an anti-Rac1 antibody. 5-10 μg of samples were loaded. Na^+/K^+ ATPase α1 subunit was immunoblotted to confirm membrane purity. (A) Rac1 localization in HG at 1 h, 3 h, 12 h. (B) Rac1 localization in 3 h HG. Src inhibitor AZD0530 (50 nM) was added 1 h before stimulation with HG. *Top,* Representative Western blot from three independent experiments is shown. *Bottom,* Stacked histograms represent densitometry of Rac1, depictied as the percentage distribution in cytosol (gray) and membrane (black). Values are the mean ± SE of three independent experiments. *, $p<0.05$ versus NG. #, $p<0.05$ versus HG. (C) In a preliminary experiment, total Rac1 was not altered by HG or Src inhibition by AZD0530.

4.02.3 Src and Rac1 co-immunoprecipitate with Vav2 in response to HG, partly dependent on Src activation

To further investigate whether high glucose activates a Src-Vav2-Rac1 pathway, the physical association of these proteins was assessed by co-immunoprecipitation. Vav2 was immunoprecipitated from primary rat MC lysates and immunoblotted for either Src or Rac1. There was a persistent increase in Src interaction with Vav2 observed at 1 h and 12 h of HG treatment (Fig. 4-4A). Similarly, Rac1 interaction with Vav2 was increased in the presence of HG and this association was blocked with AZD0530 treatment (Fig. 4-4B). These results indicate that upon HG stimulation, Src, Vav2 and Rac1 physically interact and binding of Vav2 and Rac1 is dependent on Src activation.

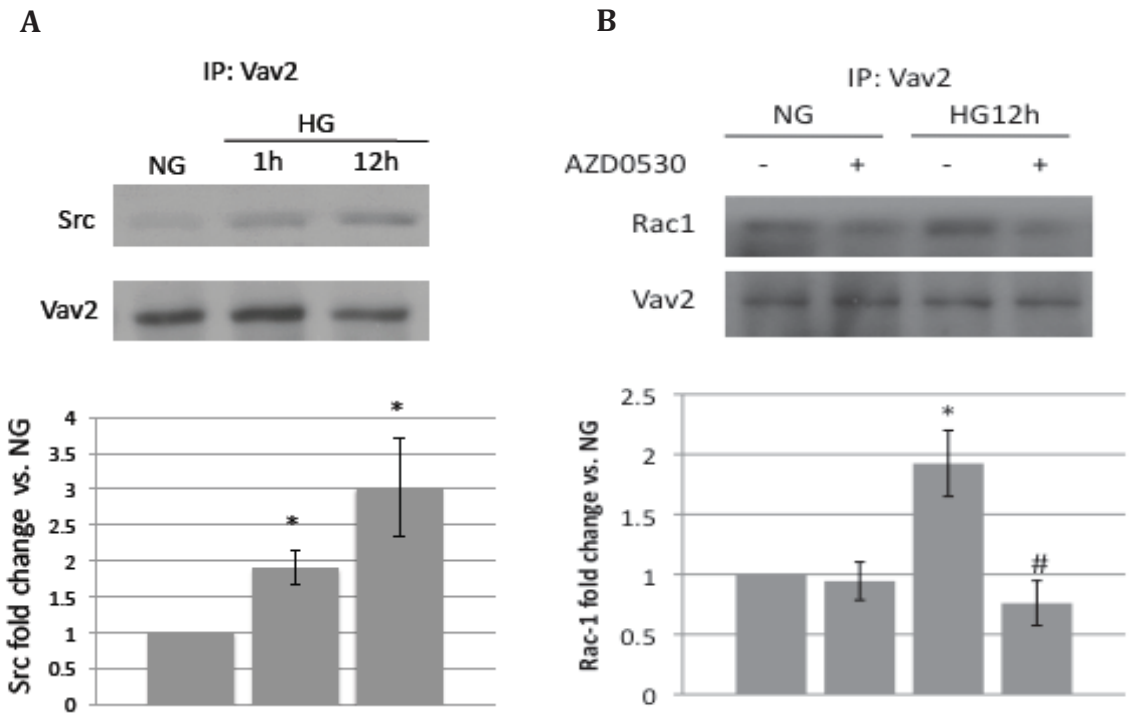

Figure 4-4. Src and Rac1 co-immunoprecipitate with Vav2 in response to high glucose. Primary rat mesangial cells were serum starved for 48 h and incubated in normal glucose (NG; 5mM) or high glucose (HG; 25mM). 1000 μg of total lysates were subject to immunoprecipitation using an anti-Vav2 antibody. (A) Immunoprecipitates were blotted with an anti-Src antibody. (B) Immunoprecipitates were blotted with anti-Rac1 antibody. Src inhibitor AZD0530 (50nM) was added 1h before stimulation with HG for 12 h. Total Vav2 expression was included as a loading control. *Top,* Representative Western blot. *Bottom,* Histograms represent the ratio of the intensity of the (A) Src band or (B) Rac1 band to the Vav2 band quantified by densitometry. Data are expressed as fold change of NG. Values are the mean ± SE (n=3). *, $p<0.05$ versus NG. #, $p<0.05$ versus HG

4.03 The role of Rac1 in HG-mediated ROS production

To assess whether Rac1 is involved in ROS production by HG, EHT1864, a chemical inhibitor of Rac1 was used in DCF and DHE fluorescence assays. Characterization studies of EHT1864 revealed that this compound binds Rac1 with high affinity, as well as related members Rac1b, Rac2 and Rac3. EHT1864 maintains Rac in an inactive state by interfering with guanine nucleotide exchange [133]. Based on this

study, a concentration of 2 μM was used and the inhibitory effect was assessed (Appendix. Fig. 7-3). Under confocal microscopy for DCF, EHT1864 blocked ROS production at 3 h and 48 h HG, although to a lesser extent at 48 h (Fig. 4-5A). When a similar experiment was performed using DHE, EHT1864 blocked ROS production at 3 h HG but not at 48 h HG. This suggests that ROS generation at longer exposure to HG may be less dependent on the activity of Rac1. Thus, ROS production appears to be dependent on Rac1 activity in short-term HG exposure.

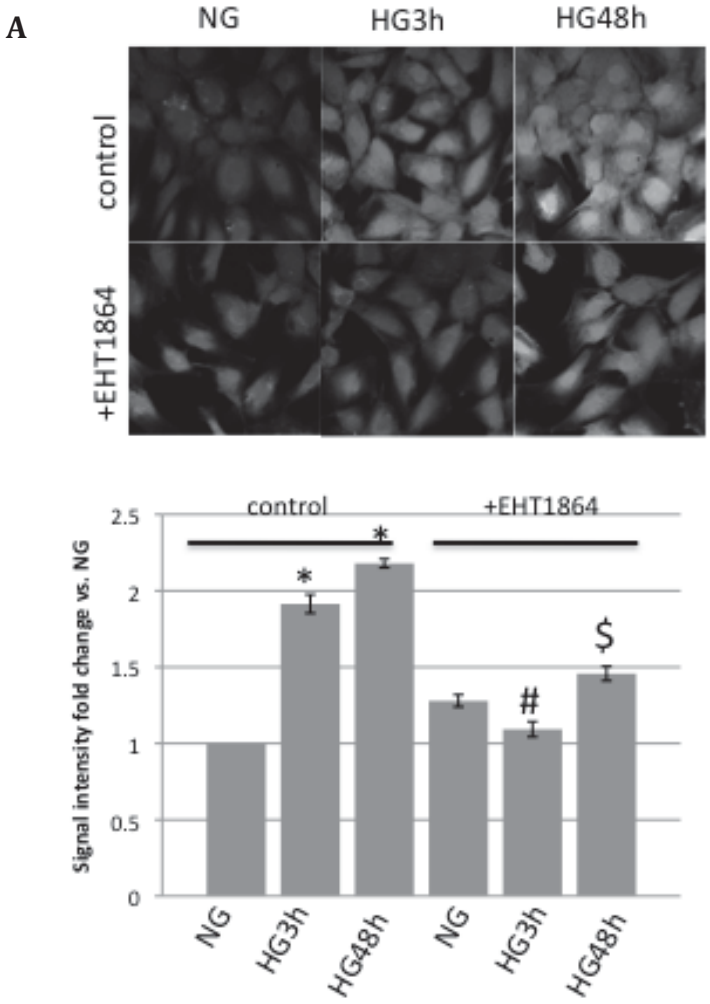

B

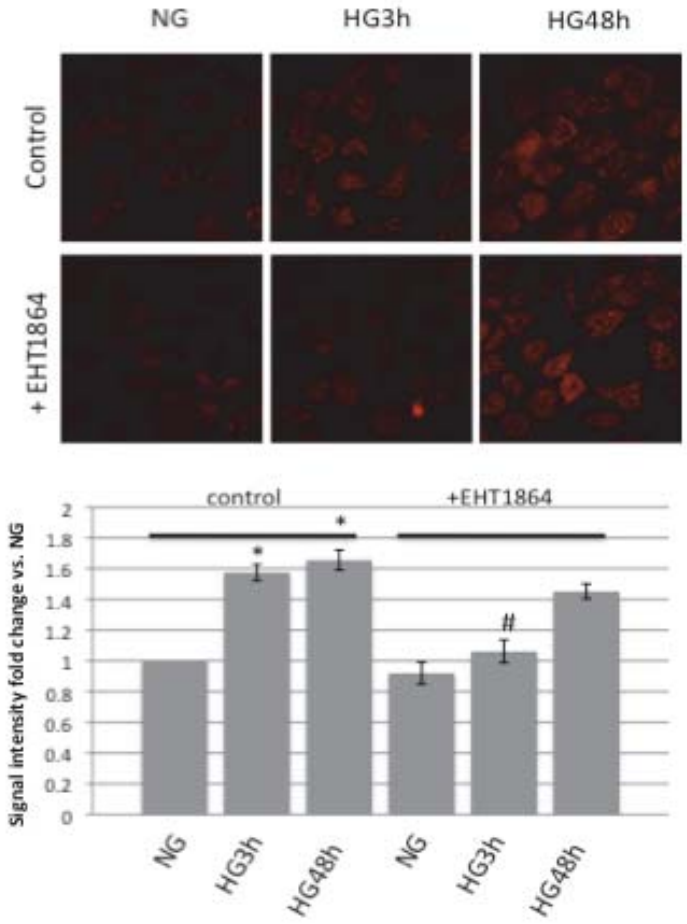

Figure 4-5. The role of Rac1 in HG-mediated ROS generation. ROS production in 3h and 48h HG assessed by DCF (A) and DHE (B). Rac1 inhibitor EHT1864 (1μM) was added 1h prior to HG treatment. *Top,* Representative micrographs showing DCF fluorescence. *Bottom,* Histograms represent the average pixel intensity per cell using ImageJ analysis. Data are expressed as fold change of NG. Values are the mean ± SE of 80-100 cells per group from three separate experiments. *, $p<0.01$ versus NG. #, $p<0.01$ versus control HG3h (without EHT), $, $p<0.01$ versus control HG48h without EHT

4.04 HG induces Nox4 protein expression mediated by Src

Given the evidence for the role of Nox4 in the diabetic kidney [47, 75, 76, 119] and that Nox4 is not regulated by Rac1 activity [68], we investigated whether Src is

required for ROS generation by Nox4 in the setting of HG. To date, reports have suggested that the activity of Nox4 may be regulated by induction of Nox4 protein expression [76]. Here, rat MCs were exposed to HG for various times and total lysates were immunoblotted for Nox4. By using a Nox4-specific siRNA, we confirmed the correct Nox4 band was at ~67 kDa, and this was the band analyzed for all experiments (Fig. 4-6D). HG increased Nox4 expression in a time-dependent manner, showing statistical significance after 12 h, 24 h and 48 h HG exposure (Fig. 4-6A). Treatment with Dasatinib, AZD0530 and Src-specific siRNA blocked Nox4 induction at 48 h HG (Fig. 4-6B and Fig. 4-6C). These results indicate that HG induces Nox4 protein expression dependent on Src activation.

A

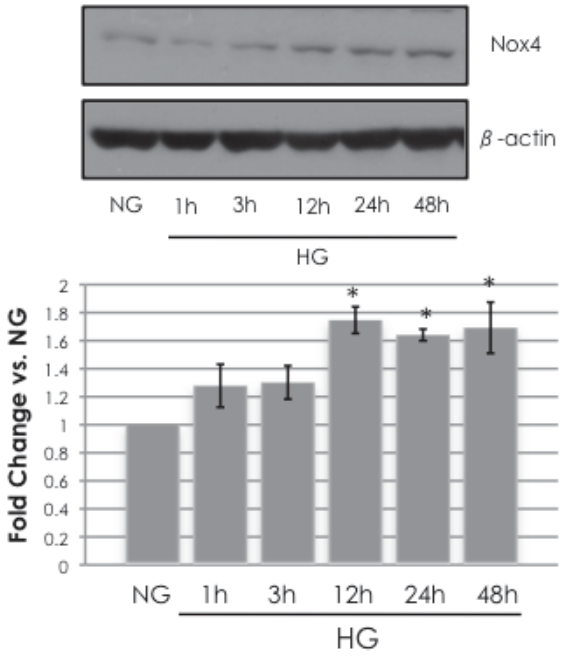

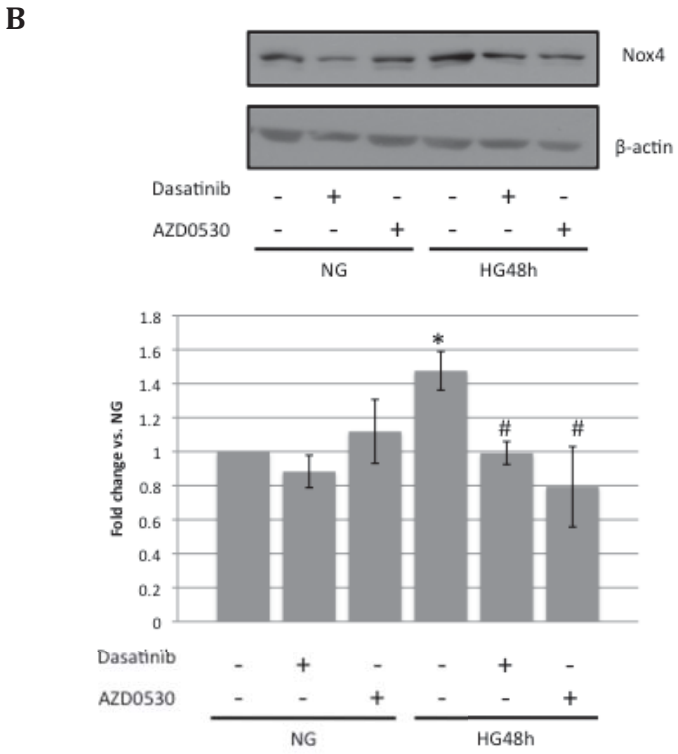
B
Nox4
β-actin
Dasatinib
AZD0530
NG
HG48h
Fold change vs. NG
1.8
1.6
1.4
1.2
1
0.8
0.6
0.4
0.2
0
*
#
#

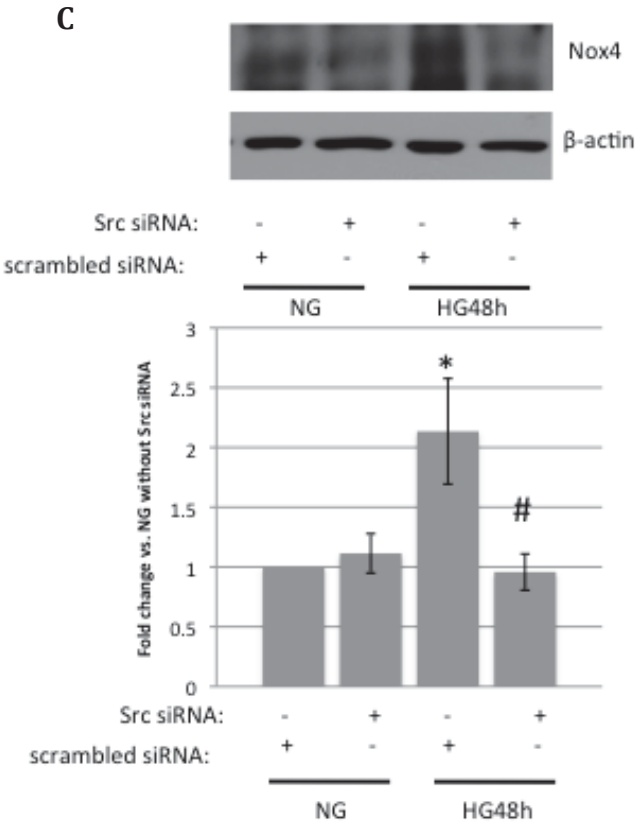
C
Nox4
β-actin
Src siRNA:
scrambled siRNA:
NG
HG48h
Fold change vs. NG without Src siRNA
3
2.5
2
1.5
1
0.5
0
*
#

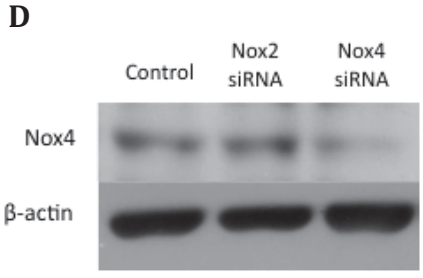
D
Control
Nox2 siRNA
Nox4 siRNA
Nox4
β-actin

Figure 4-6. Src is required for HG-induced Nox4 protein expression. Primary rat mesangial cells were serum starved for 48h and were incubated in normal glucose (NG; 5mM) or high glucose (HG; 25mM). Nox4 protein level was determined by immunoblotting 15-20μg of total lysates with anti-Nox4 antibody (Novus Biologicals). Beta-actin expression was included as a loading control. (A) Nox4 protein expression in HG at 1h, 3h, 12h, 24h and 48h. (B) Nox4 expression in 48h HG. Src inhibitors, Dasatinib (100nM) or AZD0530 (50 nM), were added 1 h before stimulation with HG. (C) Nox4 expression in 48h HG. Src-specific siRNA (2nM) or scrambled negative control siRNA (2 nM) were added for 24h, washed and followed by 48h serum starvation. (D) Nox4 protein expression in MCs transfected with control siRNA, Nox2-specific siRNA, or Nox4-specific siRNA. *Top*, Representative immunoblots. All Nox4 bands were at ~67 kDa. *Bottom*, Histograms represent densitometry of Nox4 to beta-actin. The data are expressed as fold change of NG. Values are the mean ± SE of 3-5 independent experiments. *, $p<0.05$ versus NG. #, $p<0.05$ versus HG

4.05 Differential role of Nox2 and Nox4 in HG-induced ROS production

To date, seven isoforms of the core catalytic NADPH oxidase enzyme have been discovered, each with a different expression pattern [65]. Nox1 [134], Nox2 [135] and Nox4 [76] are documented to be expressed in MCs. Many cell culture and rodent studies have demonstrated an induction of Nox4 protein, but not Nox1 or Nox2, by hyperglycemia. However, Kitada *et al.* showed increased membrane translocation and activation of $p47^{phox}$ and $p67^{phox}$ in STZ-induced diabetic rats [79]. This suggests a role of Nox1 and/or Nox2-containing NADPH oxidase in DN, since Nox1 and Nox2 but not Nox4 require these regulatory subunits [65]. In the present study, we determined the relative contributions of HG-mediated ROS generation by Nox2 and Nox4, by using Nox2- and Nox4-specific siRNAs in DCF fluorescence assays (Fig. 4-7). The knockdown efficiency and specificity of Nox siRNAs were assessed (Appendix. Fig. 7-4). After transfection and knockdown with the various siRNAs, rat MCs were exposed to HG for 1 h, 3 h, and 48 h. Interestingly, treatment with Nox2-specific siRNA only

blocked ROS production at 1 h and 3 h HG (Fig. 4-7A), while Nox4-specific siRNA only blocked ROS production at 48 h HG (Fig. 4-7B). These data suggest that ROS sources change depending on the duration of HG exposure, with early ROS generated predominantly by Nox2 while the majority of ROS after longer HG exposure are generated by Nox4.

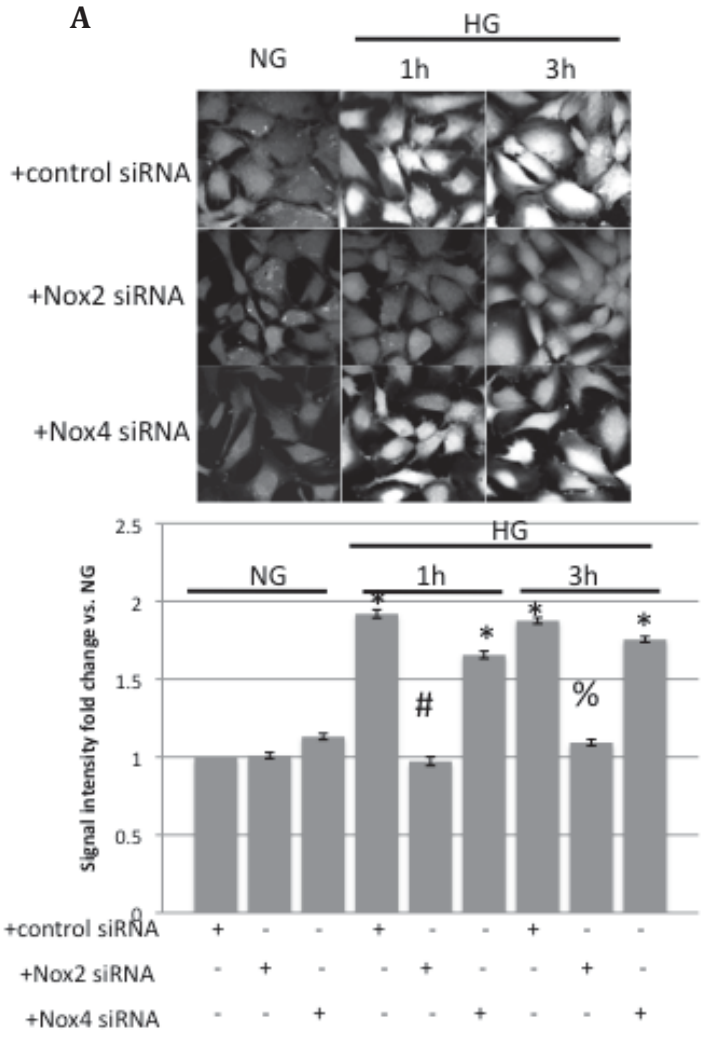

B

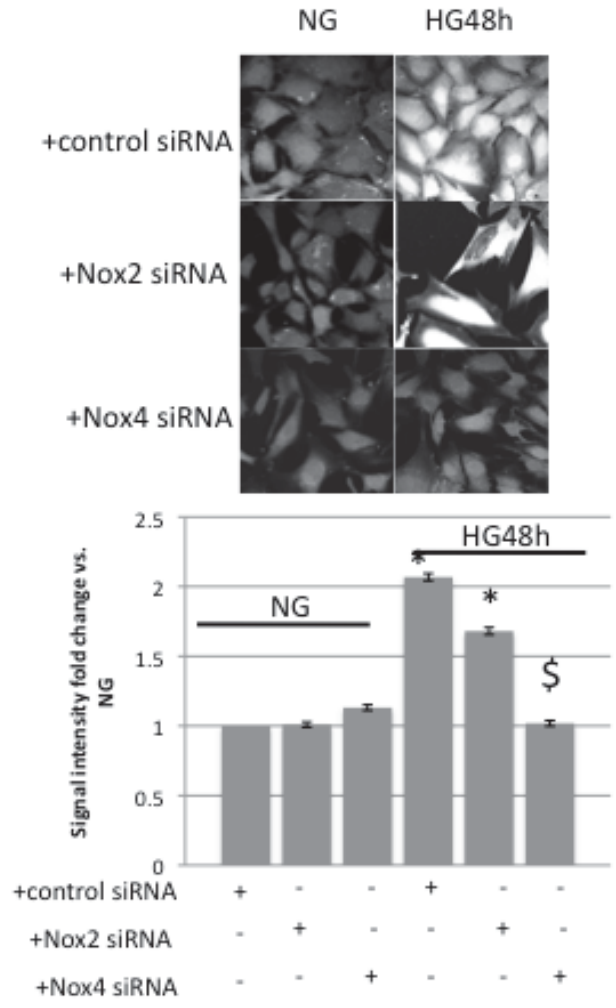

Figure 4-7. Effect of Nox2 or Nox4 knockdown on HG-induced ROS production. Primary rat mesangial cells were serum starved for 48h prior to experiments. Cells were incubated in normal glucose (NG; 5mM) or high glucose (HG; 25mM). Nox2-specific siRNA (25nM), Nox4-specific siRNA (25nM) or scrambled negative control (2nM) were added for 24h, washed and followed by 48h serum starvation (A) ROS production in 1 h and 3 h HG assessed by DCF. (B) ROS production in 48 h HG assessed by DCF. *Top,* Representative micrographs showing DCF fluorescence. *Bottom,* Histograms represent the average pixel intensity per cell using ImageJ analysis and data are expressed as fold change of NG. Values are the mean ± SE of 80-100 cells per group from three separate experiments. *, $p<0.01$ versus NG. #, $p<0.01$ versus 1 h HG, scrabled siRNA, %, $p<0.01$ versus 3 h HG, scrambled siRNA, $, $p<0.01$ versus 48 h HG, scrambled siRNA

CHAPTER 5

DISCUSSION

Chapter 5. Discussion

5.01 Summary of results

Based on evidence presented here, we propose that Src is a critical mediator of HG-induced ROS overproduction, potentially by two different mechanisms, in the model of primary cultured rat MCs (Fig. 2-1). We showed that inhibition of Src, by both chemical inhibitors and Src-specific siRNA, attenuated ROS production induced by HG. This was first demonstrated by DCF fluorescence under confocal microscopy (Fig. 4-1 A-B), however this assay has specific limitations whereby signal intensity may not correlate perfectly with ROS levels. DCF fluorescence intensity may also depend on the degree of probe retention during experimentation, governed by initial loading of the dye into cells via intracellular esterases and efflux of the dye by anion channels [136, 137]. In interpreting our DCF results, we have to be cautious that different experimental treatments may affect these underlying variables, which in turn would affect DCF fluorescence. As such, we provided further evidence by two additional methods of ROS detection: DHE fluorescence and NADPH oxidase activity (Fig 4-1 C-E). Importantly, MCs transfected with Src-specific siRNA completely normalized ROS production at both 3 h and 24 h HG exposure (Fig. 4-1B). This suggests that Src may be an upstream mediator leading to the production of ROS in both short- and long-term HG exposure.

We next investigated the mechanism of HG-induced ROS generation, as mediated by Src. We showed that Src rapidly activated a downstream Vav2-Rac1 axis leading to the generation of ROS by Rac1-dependent NADPH oxidase. HG exposure

phosphorylated and activated Vav2, and this effect was blocked by both chemical inhibitors of Src and Src-specific siRNA (Fig 4-2). We also showed that inhibiting Src with AZD0530 blocked HG-induced Rac1 membrane translocation and activation (Fig. 4-3). Indeed, blocking Rac1 activity by using the chemical inhibitor, EHT1864 attenuated ROS production induced by HG at 3 h (Fig. 4-5). To further characterize this pathway, we demonstrated that HG exposure led to increased protein-protein interactions between Src, Vav2 and Rac1. The increased association of Vav2 and Rac1 induced by HG was blocked when MCs were pre-treated with the Src inhibitor AZD0530, indicating upstream Src activity was required for mediating signaling between Vav2 and Rac1 (Fig. 4-4). Whether AZD0530 also blocks HG-induced interaction between Src and Vav2 is currently under investigation. Data from this experiment would provide insight as to whether ATP analogues, such as AZD0530, blocks substrate binding in addition to inhibiting Src kinase activity. It is well established that Rac1 is a required regulatory subunit for some members of NADPH oxidase, namely Nox1, Nox2 and Nox3 [113]. Here, we investigated whether Nox2, an isoform known to be expressed in MCs [78], was involved in HG-mediated ROS production. Knockdown of Nox2 using siRNA attenuated ROS generation in HG, at least in 1 h and 3 h exposure (Fig. 4-7A). This result was consistent with the observation that Rac1 inhibition was most effective in blocking ROS at 3 h HG, yet showed attenuation of ROS at 48 h HG only incompletely (Fig. 4-5). Together, these results suggest that short-term HG exposure activates a Src-Vav2-Rac1 pathway leading to ROS production by Nox2-containing NADPH oxidase.

Dr. Hanna Abboud's laboratory has demonstrated a critical role of Nox4 in the diabetic kidney as well as in MCs stimulated by HG [47, 75, 76, 119]. However, Nox4 is

a constitutively active isoform and does not require Rac1 as a regulatory subunit. Thus, Abboud's group demonstrated an increase in Nox4 protein upon exposure to HG [76]. To address this issue in our studies, we sought to determine whether in these experiments HG exposure increased Nox4 protein levels and to investigate whether Src was involved in this induction. Our data indicate that Nox4 protein was induced, but only after long-term (12 h to 48 h) HG exposure (Fig. 4-6A). Inhibition of Src by chemical inhibitors and by Src-specific siRNA blocked Nox4 protein induction at 48 h HG (Fig. 4-6B and Fig.4-6C). Finally, transfection with Nox4-specific siRNA led to attenuation of ROS production at 48 h HG, but not at 1 h and 3 h (Fig. 4-7). Together, these results indicate that Nox4 upregulation requires a longer duration of exposure to HG and contributes to ROS generation in chronic HG exposure.

5.02 Activation of Src by HG

As demonstrated by previous data from our lab, Src activation was observed as early as 1 h after HG exposure, and maintained for 48 h HG (Appendix Fig. 7-1A). The exact mechanism of how HG activates Src is currently unclear, but we suspect multiple signals may be involved for acute and chronic activation of Src (Fig. 5-1). Brandt *et al.* have previously demonstrated in vascular smooth muscle cells that PKC-δ leads to phosphorylation and activation of PTP-α, which in turn dephosphorylates the negative regulatory Tyr-527 and activates Src [35]. Since PKC-δ is known to be activated by HG through increased *de novo* synthesis of DAG [138], we hypothesize that this may result in the activation of Src at an early stage. Preliminary data from our lab revealed that total

PTP-α protein was induced in response to HG (Data not shown), however we have not yet assessed PTP-α activity in response to HG.

Src may also be activated by HG secondary to stimulation by other growth factors (Fig. 5-1). Previous studies have shown that HG leads to the synthesis and secretion of angiotensin II [45] and TGF-β [50], and these same growth factors may subsequently activate Src ([47], [52]) through autocrine and paracrine signaling. Thus, this may represent another mechanism of HG-induced Src activation, especially in the long-term. Importantly, the convergence of signaling from multiple growth factors to Src suggests that it could represent an important therapeutic target.

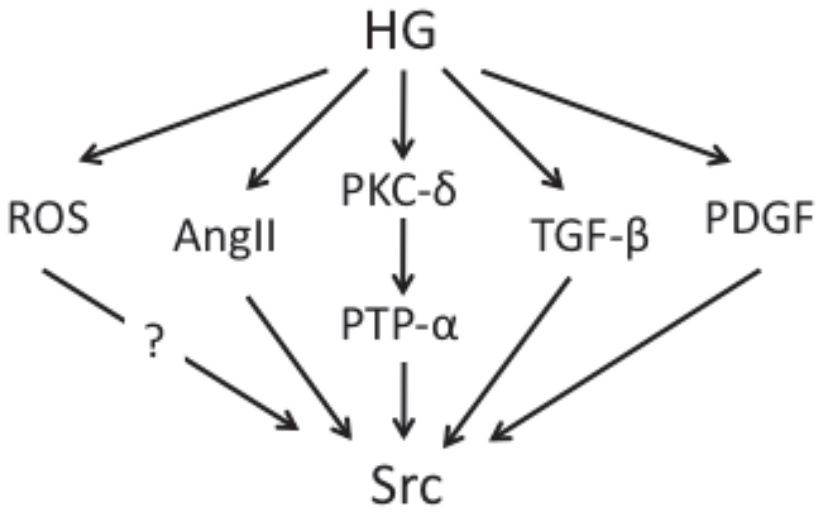

Figure 5-1. HG-induced Src activation. A schematic showing the number of possible ways that high glucose can lead to Src activation in mesangial cells. See text for details.

5.03 Mitochondrial ROS

The results presented here strongly suggest that Src activation by HG leads to ROS overproduction via NADPH oxidases, specifically Nox2 and Nox4. However, it is well known that increased glucose flux leads to mitochondrial-derived superoxide generation by the electron transport chain ([24], also see Chapter 1.03.2.1). Interestingly, our data indicate that inhibition of Src in HG almost completely normalizes ROS levels back to basal levels (Fig. 4-1). This may suggest that Src activity somehow plays a role in the mitochrondia, perhaps needed to raise the mitochondrial membrane potential over the threshold required for superoxide generation. Alternatively, Src may be involved in downregulating endogenous antioxidant enzymes and that blocking Src may result in a more reduced cellular environment. To this end, a very recent publication reported that Src subfamily kinases (Src, Fyn, and Yes) mediated nuclear export of the transcription factor Nrf2. Nrf2 binds to and enhances expression of antioxidant response element (ARE)-containing genes, including ROS scavenging enzymes such as heme oxygenase-1 (HO-1) [139]. Therefore, in MCs, blocking Src may result in enhancement of cytoprotective gene expression and defense against ROS.

While mitochondria and NADPH oxidase represent independent sources of ROS, there exists a level of cross-talk between these two systems. When HEK293T cells were stimulated by serum withdrawal, an early generation of ROS by the mitochondria was shown to be necessary for the activation of Rac1/NADPH oxidase to maintain high ROS levels [140]. In another study, NADPH oxidase-derived cytosolic ROS was necessary for the increased mitochondrial superoxide production in the context of HG. General inhibition of NADPH oxidase with apocynin abrogated mitochondrial superoxide production [141]. These studies reveal that ROS from one system may have an activating

effect on the other, and this may explain why blocking Src in our model (and thereby blocking NADPH oxidase) might also attenuate mitochondrial-derived ROS resulting in a near-complete normalization of HG-induced ROS.

5.04 Nox4 induction

We demonstrated that Nox4 protein expression was induced in MCs exposed to long-term HG (12 h to 48 h). Treatment with Src chemical inhibitors or Src-specific siRNA attenuated this effect, suggesting that Src is a critical upstream mediator of Nox4 induction (Fig. 4-6). Whether Src mediates this induction through decreased Nox4 mRNA/protein turnover, or increased transcriptional activity of the Nox4 gene remains unclear.

There have been recent reports on the Nox4 promoter being responsive to transcription factors such as Nrf2 [142], HIF-1α [143] and NFκB [144]. Pendyala *et al.* showed in lung endothelial cells that the Nox4 promoter contained AREs, binding sites for Nrf2, and that hyperoxia upregulated Nox4 gene expression via Nrf2 [142]. Interestingly, Niture *et al.* revealed that Src subfamily kinases appear to negatively regulate ARE-containing genes by mediating Nrf2 export out of the nucleus [139]. This would result in the opposite effect of what was observed here. It is not clear whether this mechanism exists in MCs in the context of HG, but if so, Src may activate other positive transcriptional regulators of Nox4 (ie. HIF-1α, NFκB) that overcome this Nrf2 deficiency. Indeed, Src has previously been implicated in the activation of HIF-1α, mediated by Rac1-dependent NADPH oxidase activity through ROS [145]. While these data are consistent with our findings in which Rac1/Nox2-containing NADPH oxidase

generated early ROS induced by HG, the observations that Rac1 inhibition and Nox2 siRNA failed to block late ROS production do not support a HIF-1α activation by this pathway. HG also elevates NFκB activity in mesangial cells [146], but whether this effect is mediated by Src in this context remain to be explored.

5.05 Effect of ROS on Src

There have been a number of reports demonstrating Src to be redox-sensitive, and in our current model of Src-mediated ROS production in HG, the resulting ROS may modulate Src function in a feedback loop. However, the exact role of ROS on Src activity remains controversial (Fig. 5-1). In a study using purified Src *in vitro*, Kemble *et a*l. showed that H_2O_2 can reverse Src activation by the reducing agent dithiothreitol (DTT) over time, but H_2O_2 alone had no effect. This suggests that the absence of a reducing agent alone was sufficiently oxidizing to cause Src inactivation. They subsequently characterized Cys-277 as the residue responsible for Src redox sensitivity, as oxidation-resistant C277A Src mutants showed elevated activity in the absence of DTT [147]. These data strongly demonstrate a negative regulatory function of oxidants on purified Src enzyme, however this effect of redox state may not adequately reflect intracellular events as ROS can modulate Src indirectly by altering upstream phosphatases and/or receptors. One example consistent with inhibition of Src by ROS was reported in cell culture studies which showed that H_2O_2 transiently inhibits Src (< 10 min) by inactivation of SHP-2, a protein tyrosine phosphatase which dephosphorlyates Src at the negative regulatory Tyr-527 [59].

In contrast, other reports have demonstrated a role for ROS in positively upregulating Src activity. In NIH 3T3 cells, oxidation of Src led to enzyme activity and this was required for anchorage-dependent cell growth and invasion [148]. Also, oxidant-resistant C245A and C487A Src mutants were not activated upon cell adherence, and failed to mediate downstream tumorigenic properties [148]. A more relevant study in MCs indicated that Nox4-derived ROS oxidizes and activates Src, leading to downstream fibronectin expression and hypertrophy. This study also implicates Cys-487 to be an important redox sensitive residue, as the C487A Src mutant prevented MC hypertrophy and fibronectin expression [47]. Combined with our data in the present study, this would place Src both upstream and downstream of ROS and specifically Nox4, again suggesting the possibility of a positive feedback loop.

From these inconsistent results, it is likely that redox regulation of Src may depend on a multitude of factors including timing of oxidant treatment, access to particular cysteine residue, cell type, and ROS modulation of molecular targets other than Src itself. From our MC model, we observed a gradual activation of Src peaking at 12 h HG, the declining somewhat by 48 h HG, although Src was still significantly activated when compared to NG (Appendix Fig. 1). Src-mediated ROS feeding back to inhibit activating PTPs (ie. SHP-2) or Src itself may explain this later effect. More importantly, in our previous studies of STZ-induced diabetic mice, Src was significantly activated in the kidney after sustained hyperglycemia for four to six weeks. This suggests that despite possible negative feedback by ROS on Src activity, chronic hyperglycemia in an animal model maintains long term Src activation, which subsequently leads to some of the pathological changes in DN (unpublished).

5.06 Conclusion

DN is a major cause of morbidity and mortality and no effective treatment is available. Advances in prevention and therapy will result from elucidation of the mechanisms and identification of specific therapeutic targets. ROS have been implicated as important mediators of diabetic kidney disease. Here, we present evidence that Src plays a key role in HG-induced ROS generation in primary rat MCs. In short-term HG exposure, Src induces Vav2 phosphorylation/activation leading to Rac1-dependent, Nox2-containing NADPH oxidase activation. In long-term HG exposure, Src induces Nox4 protein expression leading to ROS generation after the activation of Nox2-containing NADPH oxidase. These *in vitro* results are consistent with our ongoing animal studies whereby blocking Src via pharmacological intervention slows the progression of DN. In light of the current data, beneficial effects of Src blockade may in part be due to attenuation of ROS generation in the diabetic kidney.

CHAPTER 6

FUTURE DIRECTIONS

Chapter 6. Future Directions

6.01 Further Characterization of Proposed Pathway

6.01.1 *In vitro* experiments

Here, we proposed that HG activates a Src-Vav2-Rac1 pathway leading to the production of ROS by Nox2-dependent NADPH oxidase (Fig. 2-1). Indeed, there are additional experiments that can be conducted in order to provide stronger evidence for this mechanism, due to SFKs Yes and Fyn, as discussed below. Specifically, Src siRNA (5 nM) can be used to validate results with Src inhibitors in cytosol-membrane fractionation, and co-immunoprecipitation experiments. If Src siRNA transfection blocks HG-mediated Rac1 membrane translocation/activation and/or protein-protein interaction between Vav2 and Src, this would strongly suggest Src to be responsible for these downstream signaling events. In addition, inhibition of the more downstream target Vav2 and assessing that effect on HG-mediated Rac1 activation and ROS production would further characterize our proposed pathway. This can be done by transfecting MCs with Vav2-specific siRNA (Invitrogen Life Technologies). We expect siRNA knockdown of Vav2 to attenuate Rac1 activation and ROS production.

As mentioned previously, SFK members Src, Fyn and Yes are ubiquitously expressed [88], and recent data from our lab indicate Fyn and Yes protein to be present in MCs (data not shown). In order to investigate whether Fyn and/or Yes play a similar role

as Src in our proposed pathway, we will check if HG leads to their phosphorylation/activation by specifically immunoprecipitating Fyn or Yes, followed by immunoblot with a phosphospecific SFK Tyr-416 antibody. Fyn- and Yes- specific siRNA will also be used in the context of HG and several experimental outcomes assessed such as ROS production, Vav2 and Rac1 activation. If our proposed model is indeed true and HG activation of Src specifically leads to downstream signaling, we expect Fyn and Yes siRNAs to have minimal effect in blocking early Vav2/Rac1 activation, Nox4 induction and ROS production stimulated by HG.

A previous study has demonstrated Nox1 expression in MCs [134], and this may also play a role in ROS generation in response to HG. We will transfect MCs with Nox1-specific siRNA (Invitrogen) and assess HG-induced ROS generation using DCF and/or DHE. If Nox1-specific siRNA blocks ROS production in HG, this would suggest Nox1 to be involved in HG-induced ROS generation. Indeed, Nox1 is regulated similarly to Nox2 in that both isoforms require Rac1 for enzymatic activity [68]. Thus, Nox1 and Nox2 may play a similar role in the context of our proposed mechanism. If Nox1-specific siRNA does not block ROS generation in HG, this would suggest that Nox2 and Nox4, but not Nox1, are the critical isoforms involved in HG-mediated ROS production.

6.01.2 *In vivo* experiments

To determine the physiological relevance of our proposed mechanism, kidney samples from DBA/2J mice will be analyzed. Control mice and STZ-induced diabetic mice were each divided into two groups, one treated with Src inhibitor (Dasatinib or PP2) and one treated with vehicle. We obtained preliminary data demonstrating increased

Vav2 phosphorylation in diabetic mice as compared to control, and that this was attenuated in Dasatinib-treated mice. Similarly, diabetic mice showed increased Nox4 protein expression that was also blocked with Dasatinib treatment. These results support our *in vitro* data showing that Src is required for HG-induced Vav2 phosphorylation/activation (Fig. 4-2) and Nox4 induction (Fig. 4-6). We will also investigate ROS production in renal tissues by utilizing anti-4-hydroxy-2-nonenal (4-HNE) antibodies. 4-HNE is an aldehyde end-product of lipid peroxidation induced by ROS [60], and have previously been used as a marker for oxidative stress in the kidney [149, 150] Using a monoclonal antibody against 4-HNE, we will perform immunohistochemistry on paraffin-embedded kidney sections and western blotting with kidney homogenates. To correlate with our findings, we would expect increased 4-HNE staining in kidney sections from STZ-treated diabetic mice versus control, and that treatment with Dasatinib or PP2 would ameliorate this effect.

6.02 ROS as a positive feedback regulator

6.02.1 *In vitro* experiments

As previously described, ROS represents a secondary messenger capable of altering signaling cascades by oxidizing redox-sensitive targets. In our proposed model, HG stimulates early ROS generation through Nox2 while late ROS generation appear to be derived from increased Nox4. Since both of these events require Src, it is possible that they are sequentially linked and that the early-generated ROS by Nox2 in response to Src is required for the induction of Nox4 protein. Nox2 siRNA decreased but did not

completely block late ROS production by HG. To investigate this, we will perform Western blot analysis to see whether Nox4 induction by HG is blocked by Tempol, a ROS scavenger, and/or Nox2 siRNA. If Nox2-derived ROS is required for HG-induced Nox4, we expect both Tempol and Nox2 siRNA to block Nox4 induction at 48 h HG. If Nox2 is not required, we expect Nox2 siRNA to have no effect on Nox4 induction at 48 h HG. Tempol may still have an inhibitory effect on Nox4 induction by HG, indicating that other sources of ROS may stimulate Nox4 expression, such as the mitochondria. We will also expose MCs to HG and Src-specific siRNA, and then co-treat with H_2O_2 to determine whether this can rescue Nox4 induction despite Src knockdown.

6.02.2 *In vivo* experiments

To further determine whether Nox2 is required for Nox4 induction as well as Nox4-mediated ROS generation, $Nox2^{-/-}$ mice (The Jackson Laboratory, strain B6.129S6-*Cybb*^{tm1Din}/J) and $Nox4^{-/-}$ mice [151] will be used. MCs will be isolated from the kidneys of these animals as previously described [39], and exposed to HG followed by western blotting for Nox4 and assessing ROS production using DCF and/or DHE. If Nox2 is required for Nox4 induction, we would expect that in $Nox2^{-/-}$ MCs, HG exposure would either not increase Nox4 expression, or do so to a lesser extent when compared to wild-type MCs. Similarly, $Nox2^{-/-}$ MCs would show decreased ROS production when exposed to both short- and long-term HG compared to wild-type MCs. This would correlate with our *in vitro* data showing that Nox2 siRNA partially blocked ROS production at HG 48h (Fig. 4-7). In addition, we can further confirm our data from Fig. 4-7 by assessing ROS for both $Nox2^{-/-}$ and $Nox4^{-/-}$ MCs. We expect $Nox2^{-/-}$ MCs to show partial deficiency in ROS generation at HG 48h, but would show almost complete

blockage of ROS at earlier HG exposures. We also expect Nox4$^{-/-}$ MCs to show complete deficiency in ROS generation at HG 48h.

6.03 Mechanisms of Nox4 induction

Our proposed model reveals that HG induces Nox4 expression mediated by Src, but the precise mechanism is unclear. We have data in MCs indicating that HG leads to increased Nox4 mRNA levels (data not shown). Although we cannot yet rule out an effect on mRNA stability, it is likely that Nox4 protein induction is the result of enhanced transcriptional activity. Previous studies have demonstrated that the Nox4 promoter is responsive to various transcription factors, including Nrf2, HIF-1α and NFκB (see Chapter 5.04). To determine whether Nrf2 is involved, we will perform nuclear-cytosol fractionation and Western blot for Nrf2 to assess its activation, as described by Niture *et al.* [139]. If Nrf2 mediates Src-dependent induction of Nox4 by HG, then we expect increased nuclear Nrf2 expression by HG and this would be blocked by Src inhibitors and/or Src-specific siRNA. We would also expect Nrf2-specific siRNA, available from Santa Cruz Biotechnology, and/or retinoic acid [152], previously reported to inhibit Nrf2 signaling, to attenuate HG-mediated Nox4 induction.

To determine whether HIF-1α is involved, HIF-1α total protein will be immunoblotted using MC whole cell lysates. A recent study in cultured MCs reveals that HG induced HIF-1α expression in a dose-dependent manner in normoxic conditions [153]. We will confirm these findings, and test whether Src inhibitors and/or Src-specific siRNA will block HG-mediated HIF-1α induction. Also, if HIF-1α is indeed a regulator

of HG-induced Nox4 expression, we expect inhibitors of HIF-1α, such as RX-0047 (Rexahn Pharmaceuticals) or CAY10585 (Cayman Chemicals), to block this effect.

To determine whether NFκB signaling is involved, we will immunoblot for NFκB in nuclear MC fractions and/or IκB, an endogenous inhibitor of NFκB, in whole cell lysates. Increased nuclear NFκB localization and decreased IκB are indicative of activation of the NFκB pathway [154]. HG has previously been shown to upregulate NFκB activity in MCs [146]. We will confirm these results as well as utilize Src inhibitors and/or Src-specific siRNA to determine whether Src is necessary for this activation. If NFκB is indeed a regulator of HG-induced Nox4 expression, we expect the NFκB inhibitor SN50 (EMD Chemicals) to block this effect.

Nox4 induction by HG may be regulated by any of the transcription factors described above, in addition to others that are not discussed. The most efficient method to elucidate the regulator involved in our proposed model of Src-dependent Nox4 induction would be to screen the different inhibitors mentioned (retinoic acid, RX-0047, CAY10585, SN50) and determine which one(s) have an effect in blocking Nox4 induction by HG.

CHAPTER 7

APPENDIX

Chapter 7. Appendix

7.01 HG activation of Src and inhibition of Src Tyr-416 phosphorylation by chemical inhibitors

Preliminary work performed by Ling Xia, a research associate, revealed that high glucose (HG) activates Src between 1 h to 48 h (Fig. 7-1A). This was done by exposing primary rat mesangial cells to HG (25mM) in serum-free media, and Src was immunoprecipitated from whole cell lysates using a monoclonal Src antibody. A pTyr-416 antibody against SFK was then used in Western blotting to determine Src phophorylation. To determine the efficacy of Src kinase inhibition (Fig. 7-1), primary rat mesangial cells were serum starved for 48h and were incubated in normal glucose (NG; 5mM) or HG (25mM). AZD0530 was added 1 h before stimulation with HG (Fig. 7-1B). Dasatinib was added for 1 h, 3 h, or 24 h before cell harvest (Fig. 7-1C). Src kinase Tyr-416 phosphorylation level was determined by immunoblotting 15-20 μg of total lysates with anti-SFK pTyr-416 antibody. Total Src protein expression was included as a loading control.

A

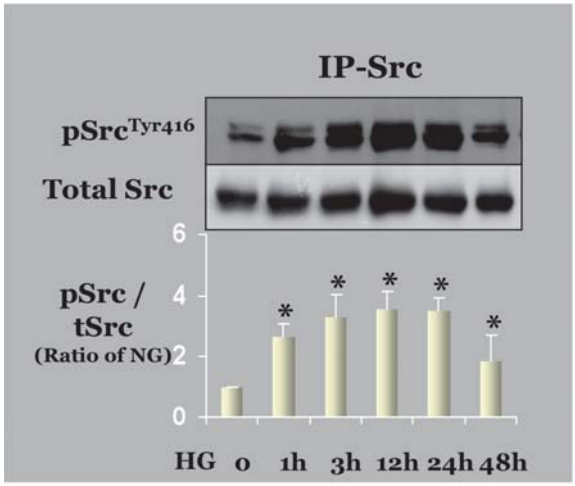

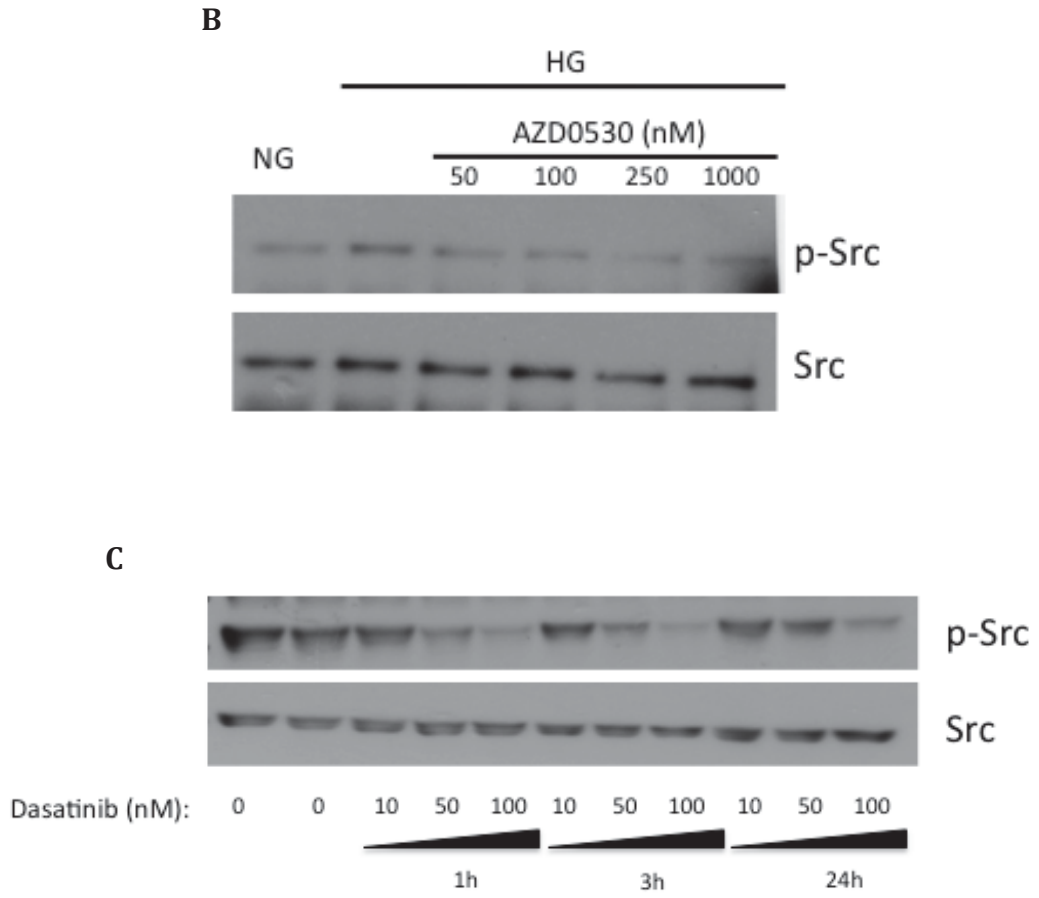

Figure 7-1. HG activation of Src and dose-dependent effect of AZD0530 (A) and Dasatinib (B) on Src Tyr-416 phosphorylation. See text for details. Fig. 7-1A was provided by Ling Xia.

7.02 Knockdown of Src by siRNA

We tested the knockdown efficiency of two different Src-specific siRNA, siRNA1 and siRNA2, in primary rat MCs (Fig. 7-2). Src siRNA1 (2 nM), Src siRNA2 (2 nM) or scrambled negative control (2 nM) were added to MCs for 24h, washed with PBS and followed by 48 h serum starvation. Cells were cultured in NG. MCs transfected with Src siRNA1 or Src siRNA 2 showed a 30% and 70% knockdown, respectively, of total Src protein when compared to control siRNA-transfected MCs (Fig. 7-2). Src siRNA2 was

used for all experiments in the present study. Total Src protein level was determined by immunoblotting 15-20 μg of total lysates with anti-Src antibody. β-actin was included as a loading control.

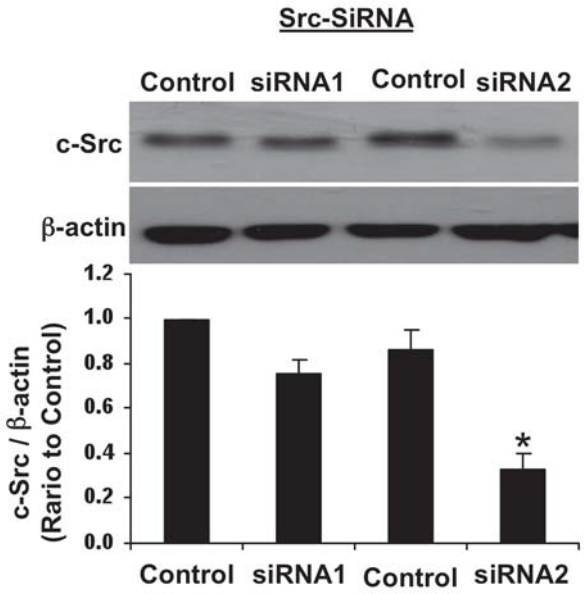

Figure 7-2. Knockdown efficiency of Src-specific siRNA on total Src protein. See text for details. *, $p<0.05$ versus control siRNA (first lane). (n=3)

7.03 Inhibition of Rac1 by EHT1864

In order to inhibit Rac1 activation, a relatively novel small molecule inhibitor EHT1864 was used. EHT1864 binds directly to Rac and interferes with guanine nucleotide exchange activity, placing Rac in an inactive state in the cytosol [133]. To assess the potency of EHT1864 (Fig. 7-3), primary rat mesangial cells were serum starved for 48 h before harvest and were incubated in normal glucose (NG; 5mM) or high glucose (HG; 25mM). MCs were pretreated with 2 μM EHT1864 for 1 h prior to HG exposure. Total lysates were subjected to ultracentrifugation to obtain cytosol and membrane fractions, followed by immunoblotting with an anti-Rac1 antibody. In the

setting of HG, EHT1864 blocked the localization of Rac1 in the membrane by 33% (Fig 7-3B). 5-10μg of samples were loaded and Na^+/K^+ ATPase α1 subunit was immunoblotted to confirm membrane purity.

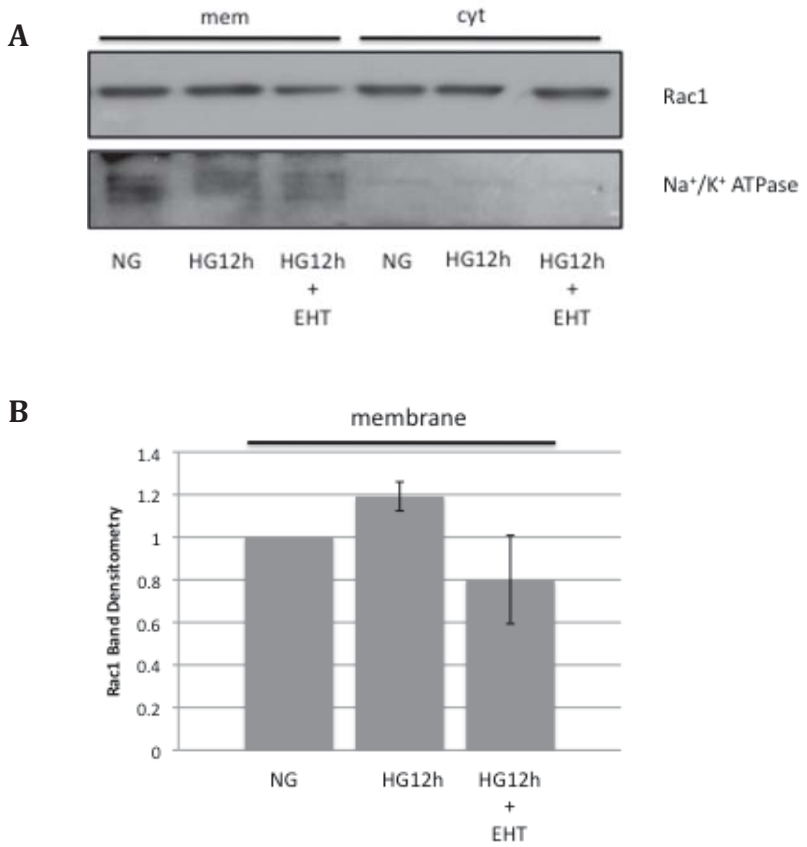

Figure 7-3. Inhibition of Rac1 translocation/activation by EHT1864. See text for details. (A) Representative immunoblot. (B) Histogram representing densitometry of Rac1 band in the membrane fraction. (n=2)

7.04 Potency and specificity of Nox2 and Nox4 siRNA

To our knowledge, there have been no previous studies elucidating the differential role of Nox isoforms in ROS generation mediated by HG. Indeed, Dr. Hanna Abboud's laboratory has demonstrated that Nox4 is a critical mediator of ROS production in DN, thereby contributing to the pathogenesis of this disease [47, 75, 76, 119]. However, there have been few studies directly showing the importance of other Nox isoforms, such as

Nox2, in such a context. In the present study, we determined the relative contributions of HG-mediated ROS by Nox2 and Nox4, by using Nox2- and Nox4-specific siRNAs in DCF fluorescence assays (Fig. 4-7). To ensure that siRNAs were effective at knocking down the specific isoform, Nox2-specific siRNA (20 nM), Nox4-specific siRNA (20 nM) or scrambled negative control (20 nM) were added for 24h, washed and followed by 48h serum starvation in normal glucose (NG; 5mM). MCs transfected with Nox4-specific siRNA, but not Nox2-specific siRNA, resulted in a 59% knockdown of Nox4 protein (Fig. 7-4A). MCs transfected with Nox2-specific siRNA, but not Nox4-specific siRNA, resulted in a 67% knockdown of Nox2 protein (Fig. 7-4B). These results indicate that the Nox siRNAs used were potent and isoform-specific. Nox2 or Nox4 proteins expression was determined by immunoblotting 15-20 μg of total lysates with anti-Nox2 or anti-Nox4 antibody. β-actin expression was included as a loading control.

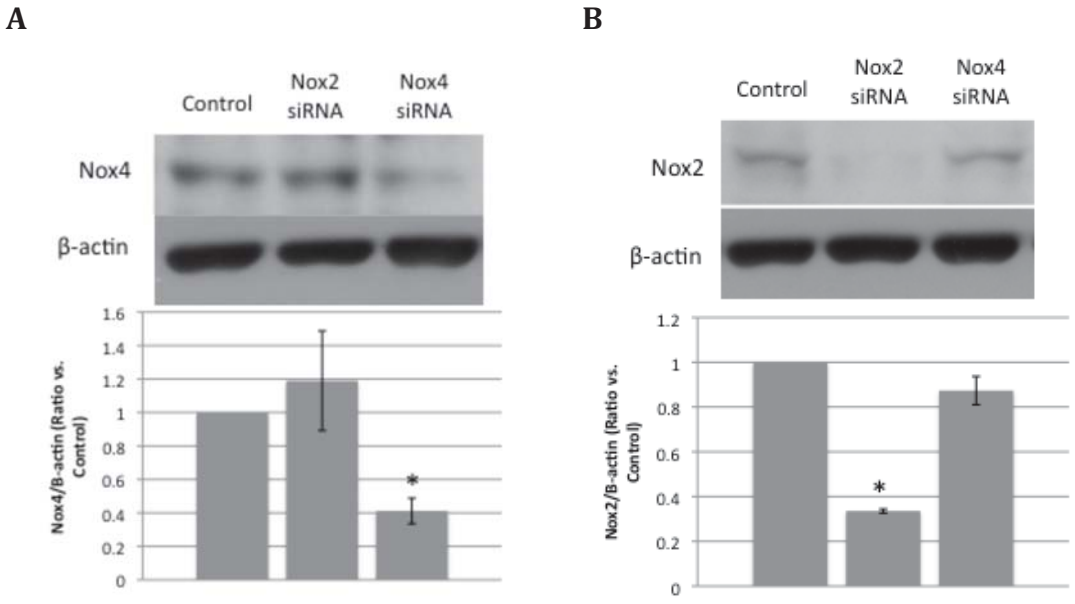

Figure 7-4. Specific knockdown of Nox2 or Nox4 by siRNA. See text for details. *, $p<0.05$ versus control siRNA (n=3-5)

CHAPTER 8

REFERENCES

Chapter 8. References

1. Wild, S., et al., *Global prevalence of diabetes: estimates for the year 2000 and projections for 2030.* Diabetes Care, 2004. **27**(5): p. 1047-53.
2. Ayodele, O.E., C.O. Alebiosu, and B.L. Salako, *Diabetic nephropathy--a review of the natural history, burden, risk factors and treatment.* J Natl Med Assoc, 2004. **96**(11): p. 1445-54.
3. Joseph, A.J. and E.A. Friedman, *Diabetic nephropathy in the elderly.* Clin Geriatr Med, 2009. **25**(3): p. 373-89.
4. Rossing, P., de Zeeuw, D., *Need for better diabetes treatment for improved renal outcome.* Kidney International, 2011. **79**(Suppl 120): p. S28-S32.
5. Najafian, B. and M. Mauer, *Progression of diabetic nephropathy in type 1 diabetic patients.* Diabetes Res Clin Pract, 2009. **83**(1): p. 1-8.
6. Falk, R.J., et al., *Polyantigenic expansion of basement membrane constituents in diabetic nephropathy.* Diabetes, 1983. **32 Suppl 2**: p. 34-9.
7. Zeisberg, M. and E.G. Neilson, *Mechanisms of tubulointerstitial fibrosis.* J Am Soc Nephrol, 2010. **21**(11): p. 1819-34.
8. Chiang, C.K. and R. Inagi, *Glomerular diseases: genetic causes and future therapeutics.* Nat Rev Nephrol, 2010. **6**(9): p. 539-54.
9. Steinke, J.M., *The natural progression of kidney injury in young type 1 diabetic patients.* Curr Diab Rep, 2009. **9**(6): p. 473-9.
10. Reddy, G.R., et al., *The podocyte and diabetes mellitus: is the podocyte the key to the origins of diabetic nephropathy?* Curr Opin Nephrol Hypertens, 2008. **17**(1): p. 32-6.
11. Eid, A.A., et al., *AMP-activated protein kinase (AMPK) negatively regulates Nox4-dependent activation of p53 and epithelial cell apoptosis in diabetes.* J Biol Chem, 2010. **285**(48): p. 37503-12.
12. Rincon-Choles, H., et al., *ZO-1 expression and phosphorylation in diabetic nephropathy.* Diabetes, 2006. **55**(4): p. 894-900.
13. Decleves, A.E. and K. Sharma, *New pharmacological treatments for improving renal outcomes in diabetes.* Nat Rev Nephrol, 2010. **6**(6): p. 371-80.
14. Wolf, G. and F.N. Ziyadeh, *Cellular and molecular mechanisms of proteinuria in diabetic nephropathy.* Nephron Physiol, 2007. **106**(2): p. p26-31.
15. Li, X., et al., *PKC-delta promotes renal tubular cell apoptosis associated with proteinuria.* J Am Soc Nephrol, 2010. **21**(7): p. 1115-24.
16. Abbate, M., C. Zoja, and G. Remuzzi, *How does proteinuria cause progressive renal damage?* J Am Soc Nephrol, 2006. **17**(11): p. 2974-84.
17. Cherney, D.Z., J.W. Scholey, and J.A. Miller, *Insights into the regulation of renal hemodynamic function in diabetic mellitus.* Curr Diabetes Rev, 2008. **4**(4): p. 280-90.
18. *The effect of intensive treatment of diabetes on the development and progression of long-term complications in insulin-dependent diabetes mellitus. The Diabetes*

Control and Complications Trial Research Group. N Engl J Med, 1993. **329**(14): p. 977-86.
19. Lewis, E.J., et al., *Renoprotective effect of the angiotensin-receptor antagonist irbesartan in patients with nephropathy due to type 2 diabetes.* N Engl J Med, 2001. **345**(12): p. 851-60.
20. Mauer, M., et al., *Renal and retinal effects of enalapril and losartan in type 1 diabetes.* N Engl J Med, 2009. **361**(1): p. 40-51.
21. Parving, H.H., et al., *Aliskiren combined with losartan in type 2 diabetes and nephropathy.* N Engl J Med, 2008. **358**(23): p. 2433-46.
22. Horie, K., et al., *Immunohistochemical colocalization of glycoxidation products and lipid peroxidation products in diabetic renal glomerular lesions. Implication for glycoxidative stress in the pathogenesis of diabetic nephropathy.* J Clin Invest, 1997. **100**(12): p. 2995-3004.
23. Daroux, M., et al., *Advanced glycation end-products: implications for diabetic and non-diabetic nephropathies.* Diabetes Metab, 2010. **36**(1): p. 1-10.
24. Brownlee, M., *Biochemistry and molecular cell biology of diabetic complications.* Nature, 2001. **414**(6865): p. 813-20.
25. Zhou, G., C. Li, and L. Cai, *Advanced glycation end-products induce connective tissue growth factor-mediated renal fibrosis predominantly through transforming growth factor beta-independent pathway.* Am J Pathol, 2004. **165**(6): p. 2033-43.
26. Yamagishi, S., et al., *Advanced glycation end product-induced apoptosis and overexpression of vascular endothelial growth factor and monocyte chemoattractant protein-1 in human-cultured mesangial cells.* J Biol Chem, 2002. **277**(23): p. 20309-15.
27. Chuang, P.Y., et al., *Advanced glycation endproducts induce podocyte apoptosis by activation of the FOXO4 transcription factor.* Kidney Int, 2007. **72**(8): p. 965-76.
28. Doublier, S., et al., *Nephrin expression is reduced in human diabetic nephropathy: evidence for a distinct role for glycated albumin and angiotensin II.* Diabetes, 2003. **52**(4): p. 1023-30.
29. Oldfield, M.D., et al., *Advanced glycation end products cause epithelial-myofibroblast transdifferentiation via the receptor for advanced glycation end products (RAGE).* J Clin Invest, 2001. **108**(12): p. 1853-63.
30. Chung, A.C., et al., *Advanced glycation end-products induce tubular CTGF via TGF-beta-independent Smad3 signaling.* J Am Soc Nephrol, 2010. **21**(2): p. 249-60.
31. Burns, W.C., et al., *Connective tissue growth factor plays an important role in advanced glycation end product-induced tubular epithelial-to-mesenchymal transition: implications for diabetic renal disease.* J Am Soc Nephrol, 2006. **17**(9): p. 2484-94.
32. Vlassara, H., et al., *Advanced glycation end products induce glomerular sclerosis and albuminuria in normal rats.* Proc Natl Acad Sci U S A, 1994. **91**(24): p. 11704-8.
33. Nakamura, S., et al., *Progression of nephropathy in spontaneous diabetic rats is prevented by OPB-9195, a novel inhibitor of advanced glycation.* Diabetes, 1997. **46**(5): p. 895-9.

34. Meier, M., J. Menne, and H. Haller, *Targeting the protein kinase C family in the diabetic kidney: lessons from analysis of mutant mice.* Diabetologia, 2009. **52**(5): p. 765-75.
35. Brandt, D.T., et al., *Protein kinase C delta induces Src kinase activity via activation of the protein tyrosine phosphatase PTP alpha.* J Biol Chem, 2003. **278**(36): p. 34073-8.
36. Whiteside, C.I. and J.A. Dlugosz, *Mesangial cell protein kinase C isozyme activation in the diabetic milieu.* Am J Physiol Renal Physiol, 2002. **282**(6): p. F975-80.
37. Studer, R.K., P.A. Craven, and F.R. DeRubertis, *Role for protein kinase C in the mediation of increased fibronectin accumulation by mesangial cells grown in high-glucose medium.* Diabetes, 1993. **42**(1): p. 118-26.
38. Thallas-Bonke, V., et al., *Inhibition of NADPH oxidase prevents advanced glycation end product-mediated damage in diabetic nephropathy through a protein kinase C-alpha-dependent pathway.* Diabetes, 2008. **57**(2): p. 460-9.
39. Kwan, J., et al., *In high glucose protein kinase C-zeta activation is required for mesangial cell generation of reactive oxygen species.* Kidney Int, 2005. **68**(6): p. 2526-41.
40. Ishii, H., et al., *Amelioration of vascular dysfunctions in diabetic rats by an oral PKC beta inhibitor.* Science, 1996. **272**(5262): p. 728-31.
41. Koya, D., et al., *Characterization of protein kinase C beta isoform activation on the gene expression of transforming growth factor-beta, extracellular matrix components, and prostanoids in the glomeruli of diabetic rats.* J Clin Invest, 1997. **100**(1): p. 115-26.
42. Tuttle, K.R., et al., *Kidney outcomes in long-term studies of ruboxistaurin for diabetic eye disease.* Clin J Am Soc Nephrol, 2007. **2**(4): p. 631-6.
43. Higuchi, S., et al., *Angiotensin II signal transduction through the AT1 receptor: novel insights into mechanisms and pathophysiology.* Clin Sci (Lond), 2007. **112**(8): p. 417-28.
44. Mima, A., et al., *Angiotensin II-dependent Src and Smad1 signaling pathway is crucial for the development of diabetic nephropathy.* Lab Invest, 2006. **86**(9): p. 927-39.
45. Singh, R., et al., *Mechanism of increased angiotensin II levels in glomerular mesangial cells cultured in high glucose.* J Am Soc Nephrol, 2003. **14**(4): p. 873-80.
46. Jaimes, E.A., J.M. Galceran, and L. Raij, *Angiotensin II induces superoxide anion production by mesangial cells.* Kidney Int, 1998. **54**(3): p. 775-84.
47. Block, K., et al., *Nox4 NAD(P)H oxidase mediates Src-dependent tyrosine phosphorylation of PDK-1 in response to angiotensin II: role in mesangial cell hypertrophy and fibronectin expression.* J Biol Chem, 2008. **283**(35): p. 24061-76.
48. Kagami, S., et al., *Angiotensin II stimulates extracellular matrix protein synthesis through induction of transforming growth factor-beta expression in rat glomerular mesangial cells.* J Clin Invest, 1994. **93**(6): p. 2431-7.
49. Massague, J., *TGF-beta signal transduction.* Annu Rev Biochem, 1998. **67**: p. 753-91.

50. Isono, S., A. Tanaka, and T. Nishino, *Effects of tongue electrical stimulation on pharyngeal mechanics in anaesthetized patients with obstructive sleep apnoea.* Eur Respir J, 1999. **14**(6): p. 1258-65.
51. Ziyadeh, F.N., *Different roles for TGF-beta and VEGF in the pathogenesis of the cardinal features of diabetic nephropathy.* Diabetes Res Clin Pract, 2008. **82 Suppl 1**: p. S38-41.
52. Mishra, R., et al., *TGF-beta-regulated collagen type I accumulation: role of Src-based signals.* Am J Physiol Cell Physiol, 2007. **292**(4): p. C1361-9.
53. Di Paolo, S., et al., *High glucose concentration induces the overexpression of transforming growth factor-beta through the activation of a platelet-derived growth factor loop in human mesangial cells.* Am J Pathol, 1996. **149**(6): p. 2095-106.
54. Sharma, K., et al., *Neutralization of TGF-beta by anti-TGF-beta antibody attenuates kidney hypertrophy and the enhanced extracellular matrix gene expression in STZ-induced diabetic mice.* Diabetes, 1996. **45**(4): p. 522-30.
55. Han, D.C., et al., *Therapy with antisense TGF-beta1 oligodeoxynucleotides reduces kidney weight and matrix mRNAs in diabetic mice.* Am J Physiol Renal Physiol, 2000. **278**(4): p. F628-34.
56. Juarez, P., et al., *Soluble betaglycan reduces renal damage progression in db/db mice.* Am J Physiol Renal Physiol, 2007. **292**(1): p. F321-9.
57. Zhang, Y., et al., *Redox Control of the Survival of Healthy and Diseased Cells.* Antioxid Redox Signal, 2011.
58. Kanwar, Y.S., et al., *A glimpse of various pathogenetic mechanisms of diabetic nephropathy.* Annu Rev Pathol, 2011. **6**: p. 395-423.
59. Tang, H., et al., *Inactivation of SRC family tyrosine kinases by reactive oxygen species in vivo.* J Biol Chem, 2005. **280**(25): p. 23918-25.
60. Richter, C., J.W. Park, and B.N. Ames, *Normal oxidative damage to mitochondrial and nuclear DNA is extensive.* Proc Natl Acad Sci U S A, 1988. **85**(17): p. 6465-7.
61. Rigoulet, M., E.D. Yoboue, and A. Devin, *Mitochondrial ROS generation and its regulation: mechanisms involved in H(2)O(2) signaling.* Antioxid Redox Signal, 2011. **14**(3): p. 459-68.
62. Tahara, E.B., F.D. Navarete, and A.J. Kowaltowski, *Tissue-, substrate-, and site-specific characteristics of mitochondrial reactive oxygen species generation.* Free Radic Biol Med, 2009. **46**(9): p. 1283-97.
63. Yu, T., J.L. Robotham, and Y. Yoon, *Increased production of reactive oxygen species in hyperglycemic conditions requires dynamic change of mitochondrial morphology.* Proc Natl Acad Sci U S A, 2006. **103**(8): p. 2653-8.
64. Yu, T., B.S. Jhun, and Y. Yoon, *High-glucose stimulation increases reactive oxygen species production through the calcium and mitogen-activated protein kinase-mediated activation of mitochondrial fission.* Antioxid Redox Signal, 2011. **14**(3): p. 425-37.
65. Bokoch, G.M., et al., *Emerging evidence for the importance of phosphorylation in the regulation of NADPH oxidases.* Antioxid Redox Signal, 2009. **11**(10): p. 2429-41.

66. Leto, T.L., et al., *Targeting and regulation of reactive oxygen species generation by Nox family NADPH oxidases.* Antioxid Redox Signal, 2009. **11**(10): p. 2607-19.
67. Lee, H.B., et al., *Reactive oxygen species-regulated signaling pathways in diabetic nephropathy.* J Am Soc Nephrol, 2003. **14**(8 Suppl 3): p. S241-5.
68. Bokoch, G.M. and B.A. Diebold, *Current molecular models for NADPH oxidase regulation by Rac GTPase.* Blood, 2002. **100**(8): p. 2692-6.
69. Nisimoto, Y., et al., *The p67(phox) activation domain regulates electron flow from NADPH to flavin in flavocytochrome b(558).* J Biol Chem, 1999. **274**(33): p. 22999-3005.
70. Chowdhury, A.K., et al., *Src-mediated tyrosine phosphorylation of p47phox in hyperoxia-induced activation of NADPH oxidase and generation of reactive oxygen species in lung endothelial cells.* J Biol Chem, 2005. **280**(21): p. 20700-11.
71. Kao, Y.Y., et al., *Identification of a conserved Rac-binding site on NADPH oxidases supports a direct GTPase regulatory mechanism.* J Biol Chem, 2008. **283**(19): p. 12736-46.
72. Serrander, L., et al., *NOX4 activity is determined by mRNA levels and reveals a unique pattern of ROS generation.* Biochem J, 2007. **406**(1): p. 105-14.
73. Geiszt, M., et al., *Identification of renox, an NAD(P)H oxidase in kidney.* Proc Natl Acad Sci U S A, 2000. **97**(14): p. 8010-4.
74. Takac, I., et al., *The E-loop is involved in hydrogen peroxide formation by the NADPH oxidase Nox4.* J Biol Chem, 2011. **286**(15): p. 13304-13.
75. Gorin, Y., et al., *Nox4 NAD(P)H oxidase mediates hypertrophy and fibronectin expression in the diabetic kidney.* J Biol Chem, 2005. **280**(47): p. 39616-26.
76. Block, K., Y. Gorin, and H.E. Abboud, *Subcellular localization of Nox4 and regulation in diabetes.* Proc Natl Acad Sci U S A, 2009. **106**(34): p. 14385-90.
77. Bondi, C.D., et al., *NAD(P)H oxidase mediates TGF-beta1-induced activation of kidney myofibroblasts.* J Am Soc Nephrol, 2010. **21**(1): p. 93-102.
78. Sedeek, M., et al., *Critical role of Nox4-based NADPH oxidase in glucose-induced oxidative stress in the kidney: implications in type 2 diabetic nephropathy.* Am J Physiol Renal Physiol, 2010. **299**(6): p. F1348-58.
79. Kitada, M., et al., *Translocation of glomerular p47phox and p67phox by protein kinase C-beta activation is required for oxidative stress in diabetic nephropathy.* Diabetes, 2003. **52**(10): p. 2603-14.
80. Lee, G.T., et al., *Delayed treatment with lithospermate B attenuates experimental diabetic renal injury.* J Am Soc Nephrol, 2003. **14**(3): p. 709-20.
81. Craven, P.A., et al., *Overexpression of Cu2+/Zn2+ superoxide dismutase protects against early diabetic glomerular injury in transgenic mice.* Diabetes, 2001. **50**(9): p. 2114-25.
82. Lonn, E., et al., *Effects of vitamin E on cardiovascular and microvascular outcomes in high-risk patients with diabetes: results of the HOPE study and MICRO-HOPE substudy.* Diabetes Care, 2002. **25**(11): p. 1919-27.
83. Chiabrando, C., et al., *Long-term vitamin E supplementation fails to reduce lipid peroxidation in people at cardiovascular risk: analysis of underlying factors.* Curr Control Trials Cardiovasc Med, 2002. **3**(1): p. 5.

84. Ceriello, A. and R. Testa, *Antioxidant anti-inflammatory treatment in type 2 diabetes.* Diabetes Care, 2009. **32 Suppl 2**: p. S232-6.
85. Martin, G.S., *The road to Src.* Oncogene, 2004. **23**(48): p. 7910-7.
86. Takeya, T. and H. Hanafusa, *Structure and sequence of the cellular gene homologous to the RSV src gene and the mechanism for generating the transforming virus.* Cell, 1983. **32**(3): p. 881-90.
87. Boggon, T.J. and M.J. Eck, *Structure and regulation of Src family kinases.* Oncogene, 2004. **23**(48): p. 7918-27.
88. Sandilands, E., V.G. Brunton, and M.C. Frame, *The membrane targeting and spatial activation of Src, Yes and Fyn is influenced by palmitoylation and distinct RhoB/RhoD endosome requirements.* J Cell Sci, 2007. **120**(Pt 15): p. 2555-64.
89. Knighton, D.R., et al., *Crystal structure of the catalytic subunit of cyclic adenosine monophosphate-dependent protein kinase.* Science, 1991. **253**(5018): p. 407-14.
90. Eck, M.J., S.E. Shoelson, and S.C. Harrison, *Recognition of a high-affinity phosphotyrosyl peptide by the Src homology-2 domain of p56lck.* Nature, 1993. **362**(6415): p. 87-91.
91. Xu, W., S.C. Harrison, and M.J. Eck, *Three-dimensional structure of the tyrosine kinase c-Src.* Nature, 1997. **385**(6617): p. 595-602.
92. Brown, M.T. and J.A. Cooper, *Regulation, substrates and functions of src.* Biochim Biophys Acta, 1996. **1287**(2-3): p. 121-49.
93. Kypta, R.M., et al., *Association between the PDGF receptor and members of the src family of tyrosine kinases.* Cell, 1990. **62**(3): p. 481-92.
94. Nada, S., et al., *Cloning of a complementary DNA for a protein-tyrosine kinase that specifically phosphorylates a negative regulatory site of p60c-src.* Nature, 1991. **351**(6321): p. 69-72.
95. Zheng, X.M., Y. Wang, and C.J. Pallen, *Cell transformation and activation of pp60c-src by overexpression of a protein tyrosine phosphatase.* Nature, 1992. **359**(6393): p. 336-9.
96. Suzaki, Y., et al., *BMK1 is activated in glomeruli of diabetic rats and in mesangial cells by high glucose conditions.* Kidney Int, 2004. **65**(5): p. 1749-60.
97. Choudhury, G.G., et al., *c-Src couples PI 3 kinase/Akt and MAPK signaling to PDGF-induced DNA synthesis in mesangial cells.* Cell Signal, 2006. **18**(11): p. 1854-64.
98. Crespo, P., et al., *Phosphotyrosine-dependent activation of Rac-1 GDP/GTP exchange by the vav proto-oncogene product.* Nature, 1997. **385**(6612): p. 169-72.
99. Turner, M. and D.D. Billadeau, *VAV proteins as signal integrators for multi-subunit immune-recognition receptors.* Nat Rev Immunol, 2002. **2**(7): p. 476-86.
100. Han, J., et al., *Lck regulates Vav activation of members of the Rho family of GTPases.* Mol Cell Biol, 1997. **17**(3): p. 1346-53.
101. Swat, W. and K. Fujikawa, *The Vav family: at the crossroads of signaling pathways.* Immunol Res, 2005. **32**(1-3): p. 259-65.
102. Lopez-Lago, M., et al., *Tyrosine phosphorylation mediates both activation and downmodulation of the biological activity of Vav.* Mol Cell Biol, 2000. **20**(5): p. 1678-91.

103. Billadeau, D.D., et al., *Specific subdomains of Vav differentially affect T cell and NK cell activation.* J Immunol, 2000. **164**(8): p. 3971-81.
104. Movilla, N. and X.R. Bustelo, *Biological and regulatory properties of Vav-3, a new member of the Vav family of oncoproteins.* Mol Cell Biol, 1999. **19**(11): p. 7870-85.
105. Aghazadeh, B., et al., *Structural basis for relief of autoinhibition of the Dbl homology domain of proto-oncogene Vav by tyrosine phosphorylation.* Cell, 2000. **102**(5): p. 625-33.
106. Han, J., et al., *Role of substrates and products of PI 3-kinase in regulating activation of Rac-related guanosine triphosphatases by Vav.* Science, 1998. **279**(5350): p. 558-60.
107. Yi, F., et al., *Mechanism of homocysteine-induced Rac1/NADPH oxidase activation in mesangial cells: role of guanine nucleotide exchange factor Vav2.* Cell Physiol Biochem, 2007. **20**(6): p. 909-18.
108. Yi, F., et al., *Contribution of guanine nucleotide exchange factor Vav2 to hyperhomocysteinemic glomerulosclerosis in rats.* Hypertension, 2009. **53**(1): p. 90-6.
109. Peng, F., et al., *Mechanical stretch-induced RhoA activation is mediated by the RhoGEF Vav2 in mesangial cells.* Cell Signal, 2010. **22**(1): p. 34-40.
110. Zhang, Y., et al., *Mechanical strain-induced RhoA activation requires NADPH oxidase-mediated ROS generation in caveolae.* Antioxid Redox Signal, 2010. **13**(7): p. 959-73.
111. Wennerberg, K. and C.J. Der, *Rho-family GTPases: it's not only Rac and Rho (and I like it).* J Cell Sci, 2004. **117**(Pt 8): p. 1301-12.
112. Brown, J.H., D.P. Del Re, and M.A. Sussman, *The Rac and Rho hall of fame: a decade of hypertrophic signaling hits.* Circ Res, 2006. **98**(6): p. 730-42.
113. Bokoch, G.M. and T. Zhao, *Regulation of the phagocyte NADPH oxidase by Rac GTPase.* Antioxid Redox Signal, 2006. **8**(9-10): p. 1533-48.
114. Zhao, X., K.A. Carnevale, and M.K. Cathcart, *Human monocytes use Rac1, not Rac2, in the NADPH oxidase complex.* J Biol Chem, 2003. **278**(42): p. 40788-92.
115. Jordan, P., et al., *Cloning of a novel human Rac1b splice variant with increased expression in colorectal tumors.* Oncogene, 1999. **18**(48): p. 6835-9.
116. Griner, E.M., et al., *A novel cross-talk in diacylglycerol signaling: the Rac-GAP beta2-chimaerin is negatively regulated by protein kinase Cdelta-mediated phosphorylation.* J Biol Chem, 2010. **285**(22): p. 16931-41.
117. Diekmann, D., et al., *Interaction of Rac with p67phox and regulation of phagocytic NADPH oxidase activity.* Science, 1994. **265**(5171): p. 531-3.
118. Dentelli, P., et al., *Oxidative stress-mediated mesangial cell proliferation requires RAC-1/reactive oxygen species production and beta4 integrin expression.* J Biol Chem, 2007. **282**(36): p. 26101-10.
119. Gorin, Y., et al., *Nox4 mediates angiotensin II-induced activation of Akt/protein kinase B in mesangial cells.* Am J Physiol Renal Physiol, 2003. **285**(2): p. F219-29.
120. Lin, C.L., et al., *Superoxide destabilization of beta-catenin augments apoptosis of high-glucose-stressed mesangial cells.* Endocrinology, 2008. **149**(6): p. 2934-42.

121. Bielek, H., A. Anselmo, and C. Dermardirossian, *Morphological and proliferative abnormalities in renal mesangial cells lacking RhoGDI.* Cell Signal, 2009. **21**(12): p. 1974-83.
122. Shibata, S., et al., *Modification of mineralocorticoid receptor function by Rac1 GTPase: implication in proteinuric kidney disease.* Nat Med, 2008. **14**(12): p. 1370-6.
123. Bertocchio, J.P., D.G. Warnock, and F. Jaisser, *Mineralocorticoid receptor activation and blockade: an emerging paradigm in chronic kidney disease.* Kidney Int, 2011. **79**(10): p. 1051-60.
124. Vecchione, C., et al., *A novel mechanism of action for statins against diabetes-induced oxidative stress.* Diabetologia, 2007. **50**(4): p. 874-80.
125. Lombardo, L.J., et al., *Discovery of N-(2-chloro-6-methyl- phenyl)-2-(6-(4-(2-hydroxyethyl)- piperazin-1-yl)-2-methylpyrimidin-4- ylamino)thiazole-5-carboxamide (BMS-354825), a dual Src/Abl kinase inhibitor with potent antitumor activity in preclinical assays.* J Med Chem, 2004. **47**(27): p. 6658-61.
126. Blake, R.A., et al., *SU6656, a selective src family kinase inhibitor, used to probe growth factor signaling.* Mol Cell Biol, 2000. **20**(23): p. 9018-27.
127. Hennequin, L.F., et al., *N-(5-chloro-1,3-benzodioxol-4-yl)-7-[2-(4-methylpiperazin-1-yl)ethoxy]-5- (tetrahydro-2H-pyran-4-yloxy)quinazolin-4-amine, a novel, highly selective, orally available, dual-specific c-Src/Abl kinase inhibitor.* J Med Chem, 2006. **49**(22): p. 6465-88.
128. Chen, X., et al., *2',7'-Dichlorodihydrofluorescein as a fluorescent probe for reactive oxygen species measurement: Forty years of application and controversy.* Free Radic Res, 2010. **44**(6): p. 587-604.
129. Zielonka, J., J. Vasquez-Vivar, and B. Kalyanaraman, *Detection of 2-hydroxyethidium in cellular systems: a unique marker product of superoxide and hydroethidine.* Nat Protoc, 2008. **3**(1): p. 8-21.
130. Zielonka, J. and B. Kalyanaraman, *Hydroethidine- and MitoSOX-derived red fluorescence is not a reliable indicator of intracellular superoxide formation: another inconvenient truth.* Free Radic Biol Med, 2010. **48**(8): p. 983-1001.
131. Gianni, D., et al., *The involvement of the tyrosine kinase c-Src in the regulation of reactive oxygen species generation mediated by NADPH oxidase-1.* Mol Biol Cell, 2008. **19**(7): p. 2984-94.
132. Soumya Saha, Z.J., Dongmin Liu , and Hara P. Misra *Superoxide Anion and NADPH Oxidase Activity Determination in Vascular Smooth Muscle Cells and Tissues from Rats.* Methods in Redox Signaling, 2010.
133. Shutes, A., et al., *Specificity and mechanism of action of EHT 1864, a novel small molecule inhibitor of Rac family small GTPases.* J Biol Chem, 2007. **282**(49): p. 35666-78.
134. Pleskova, M., et al., *Nitric oxide down-regulates the expression of the catalytic NADPH oxidase subunit Nox1 in rat renal mesangial cells.* FASEB J, 2006. **20**(1): p. 139-41.
135. Oudit, G.Y., et al., *Human recombinant ACE2 reduces the progression of diabetic nephropathy.* Diabetes, 2010. **59**(2): p. 529-38.

136. Wan, X.S., Z. Zhou, and A.R. Kennedy, *Adaptation of the dichlorofluorescein assay for detection of radiation-induced oxidative stress in cultured cells.* Radiat Res, 2003. **160**(6): p. 622-30.
137. Laupeze, B., et al., *Use of the anionic dye carboxy-2',7'-dichlorofluorescein for sensitive flow cytometric detection of multidrug resistance-associated protein activity.* Int J Oncol, 1999. **15**(3): p. 571-6.
138. Haller, H., et al., *High glucose concentrations and protein kinase C isoforms in vascular smooth muscle cells.* Kidney Int, 1995. **47**(4): p. 1057-67.
139. Niture, S.K., et al., *Src subfamily kinases regulate nuclear export and degradation of the transcription factor Nrf2 to switch off Nrf2-mediated antioxidant activation of cytoprotective gene expression.* J Biol Chem, 2011.
140. Lee, S.B., et al., *Link between mitochondria and NADPH oxidase 1 isozyme for the sustained production of reactive oxygen species and cell death.* J Biol Chem, 2006. **281**(47): p. 36228-35.
141. Coughlan, M.T., et al., *RAGE-induced cytosolic ROS promote mitochondrial superoxide generation in diabetes.* J Am Soc Nephrol, 2009. **20**(4): p. 742-52.
142. Pendyala, S., et al., *Nrf2 regulates hyperoxia-induced Nox4 expression in human lung endothelium: identification of functional antioxidant response elements on the Nox4 promoter.* Free Radic Biol Med, 2011. **50**(12): p. 1749-59.
143. Diebold, I., et al., *The NADPH oxidase subunit NOX4 is a new target gene of the hypoxia-inducible factor-1.* Mol Biol Cell, 2010. **21**(12): p. 2087-96.
144. Manea, A., et al., *Transcriptional regulation of NADPH oxidase isoforms, Nox1 and Nox4, by nuclear factor-kappaB in human aortic smooth muscle cells.* Biochem Biophys Res Commun, 2010. **396**(4): p. 901-7.
145. Lee, H.Y., et al., *Src activates HIF-1alpha not through direct phosphorylation of HIF-1alpha specific prolyl-4 hydroxylase 2 but through activation of the NADPH oxidase/Rac pathway.* Carcinogenesis, 2011. **32**(5): p. 703-12.
146. Ha, H., et al., *Role of high glucose-induced nuclear factor-kappaB activation in monocyte chemoattractant protein-1 expression by mesangial cells.* J Am Soc Nephrol, 2002. **13**(4): p. 894-902.
147. Kemble, D.J. and G. Sun, *Direct and specific inactivation of protein tyrosine kinases in the Src and FGFR families by reversible cysteine oxidation.* Proc Natl Acad Sci U S A, 2009. **106**(13): p. 5070-5.
148. Giannoni, E., et al., *Intracellular reactive oxygen species activate Src tyrosine kinase during cell adhesion and anchorage-dependent cell growth.* Mol Cell Biol, 2005. **25**(15): p. 6391-403.
149. Yamazaki, T., et al., *Combination effects of enalapril and losartan on lipid peroxidation in the kidneys of KK-Ay/Ta mice.* Nephron Exp Nephrol, 2009. **113**(2): p. e66-76.
150. Kurisaki, E. and K. Hiraiwa, *Western blot analysis for 4-hydroxy-2-nonenal (HNE)-modified proteins in paraquat-treated mice.* Leg Med (Tokyo), 2009. **11 Suppl 1**: p. S431-3.
151. Garrido-Urbani, S., et al., *Targeting vascular NADPH oxidase 1 blocks tumor angiogenesis through a PPARalpha mediated mechanism.* PLoS One, 2011. **6**(2): p. e14665.

152. Wang, X.J., et al., *Identification of retinoic acid as an inhibitor of transcription factor Nrf2 through activation of retinoic acid receptor alpha.* Proc Natl Acad Sci U S A, 2007. **104**(49): p. 19589-94.
153. Isoe, T., et al., *High glucose activates HIF-1-mediated signal transduction in glomerular mesangial cells through a carbohydrate response element binding protein.* Kidney Int, 2010. **78**(1): p. 48-59.
154. Schreck, R., P. Rieber, and P.A. Baeuerle, *Reactive oxygen intermediates as apparently widely used messengers in the activation of the NF-kappa B transcription factor and HIV-1.* EMBO J, 1991. **10**(8): p. 2247-58.